

# Angular Momentum Presentation

## Week 2

from Iskenderian and Salstein, *Monthly Weather Review* (1998)

## 2. Definitions and data sources

The global atmospheric angular momentum about the earth's axis can be expressed as

$$\text{AAM} = M_r + M_\Omega, \quad (1)$$

where

$$M_r = \frac{a^3}{g} \iiint u \cos^2\phi \, d\phi \, d\lambda \, dp \quad (2)$$

is the entire atmosphere's angular momentum associated with its motion relative to the rotating solid earth,  $a$  is the earth's radius,  $g$  is acceleration due to gravity,  $u$  is zonal wind, and the integral is performed over all latitudes  $\phi$ , longitudes  $\lambda$ , and pressures  $p$ . The angular mo-

mentum associated with the rotation of the atmosphere's mass is

$$M_\Omega = \frac{a^4 \Omega}{g} \iint p_s \cos^3 \phi \, d\phi \, d\lambda, \quad (3)$$

where  $\Omega$  is the mean rotation rate of the earth and  $p_s$ , the surface pressure (Rosen 1993).

The conservation of angular momentum states that changes in AAM are related to the surface torque by the relationship

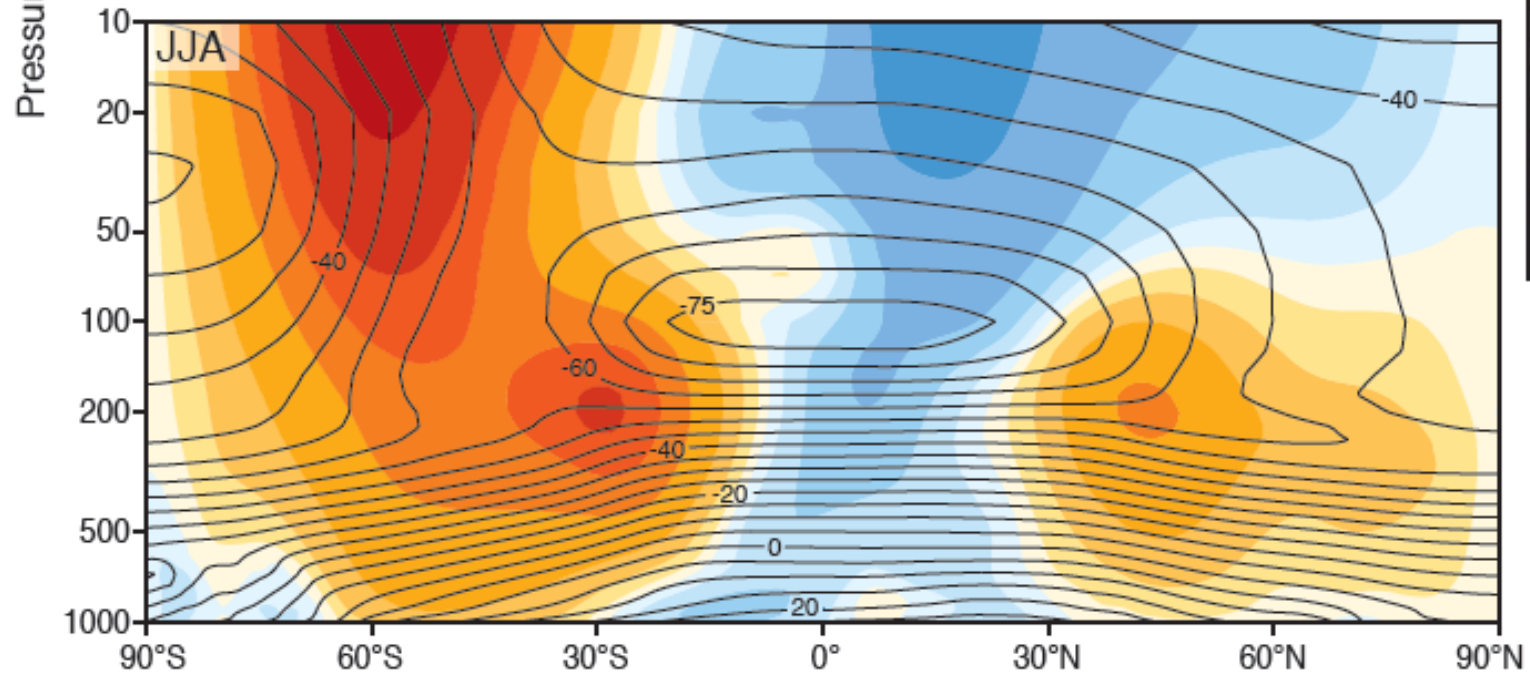
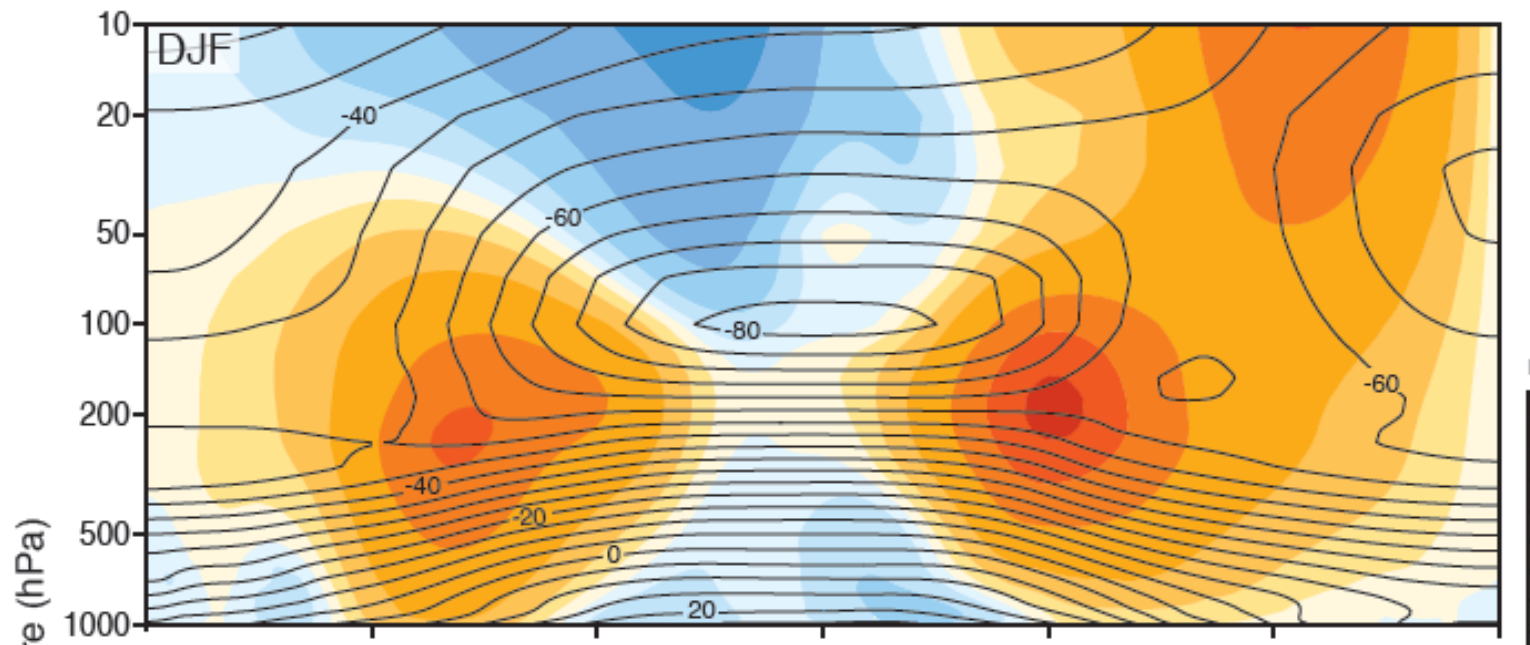
$$\frac{d}{dt} \text{AAM} = T_m + T_f, \quad (4)$$

where the mountain torque ( $T_m$ ) and friction torque ( $T_f$ ) are defined through the following relationships (White 1991):

$$T_m = -a^2 \iint p_s \frac{\partial H}{\partial \lambda} \cos \phi \, d\phi \, d\lambda, \quad (5)$$

$$T_f = a^3 \iint \tau \cos^2 \phi \, d\phi \, d\lambda. \quad (6)$$

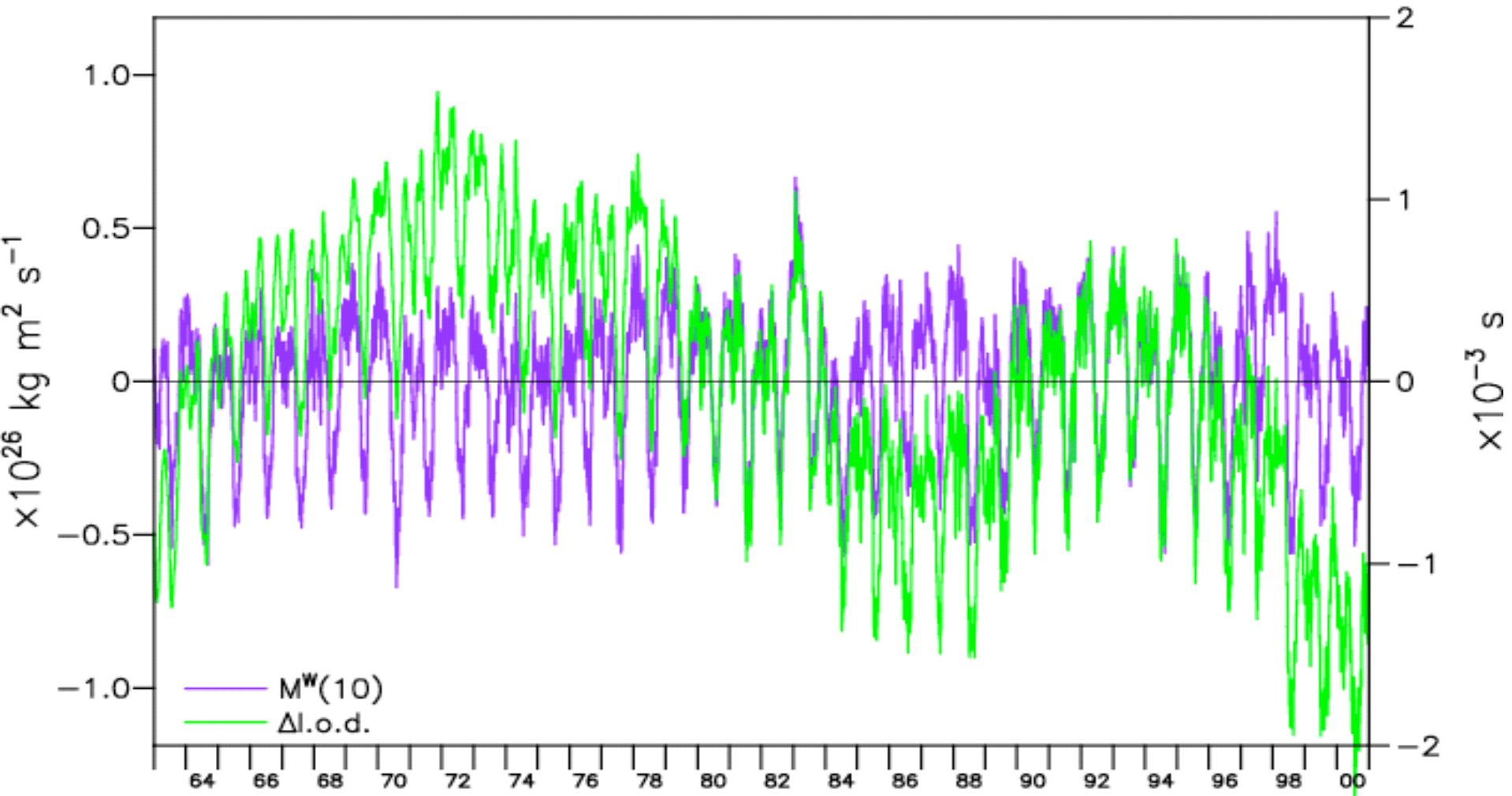
Here,  $\tau$  is surface stress and  $H$  indicates the height of the sloping topography.



J

tein

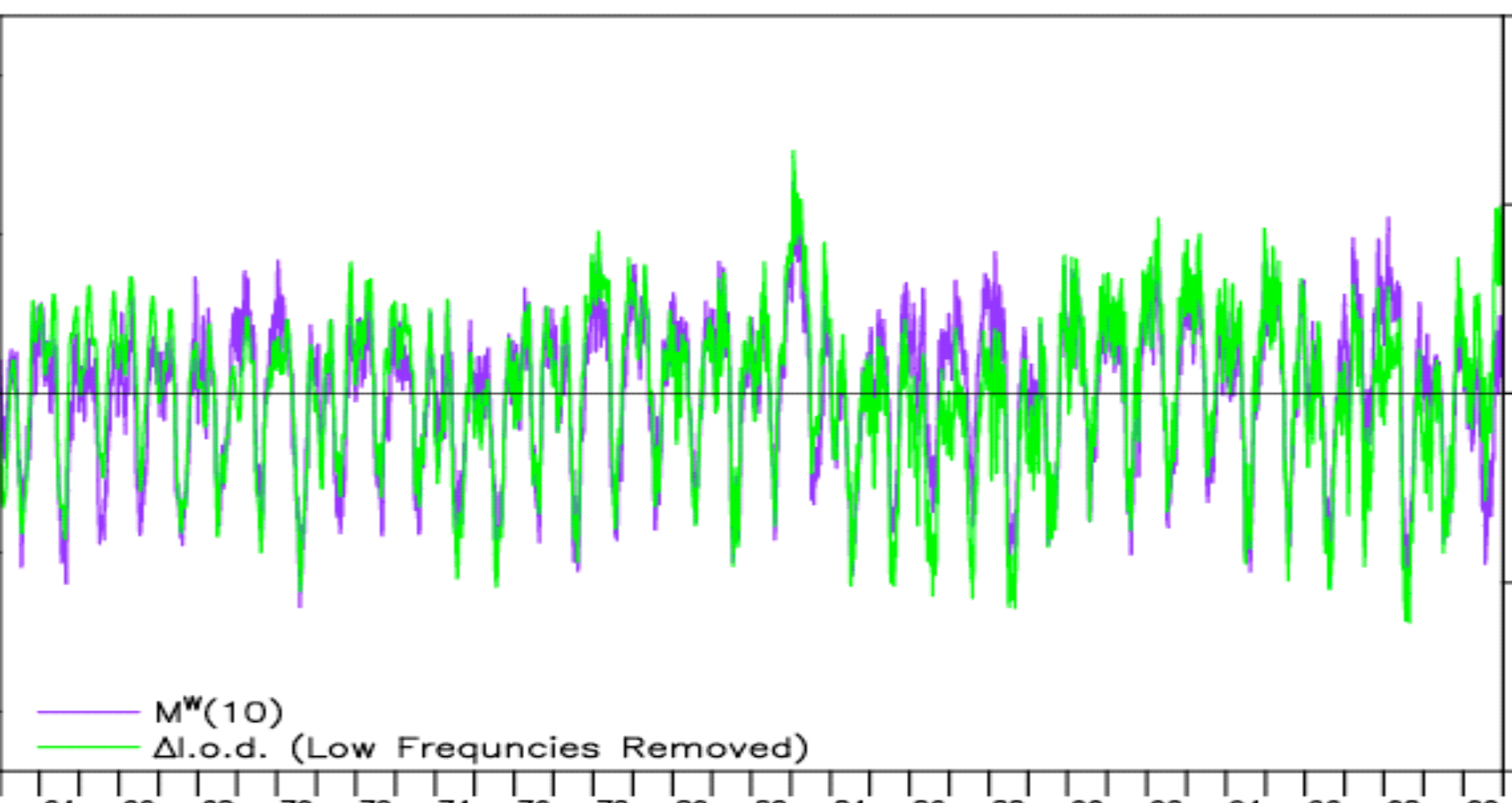
## AAM and Length of Day



$$\Delta M = k \times \Delta(\text{L.O.D.})$$

Courtesy of David Salstein

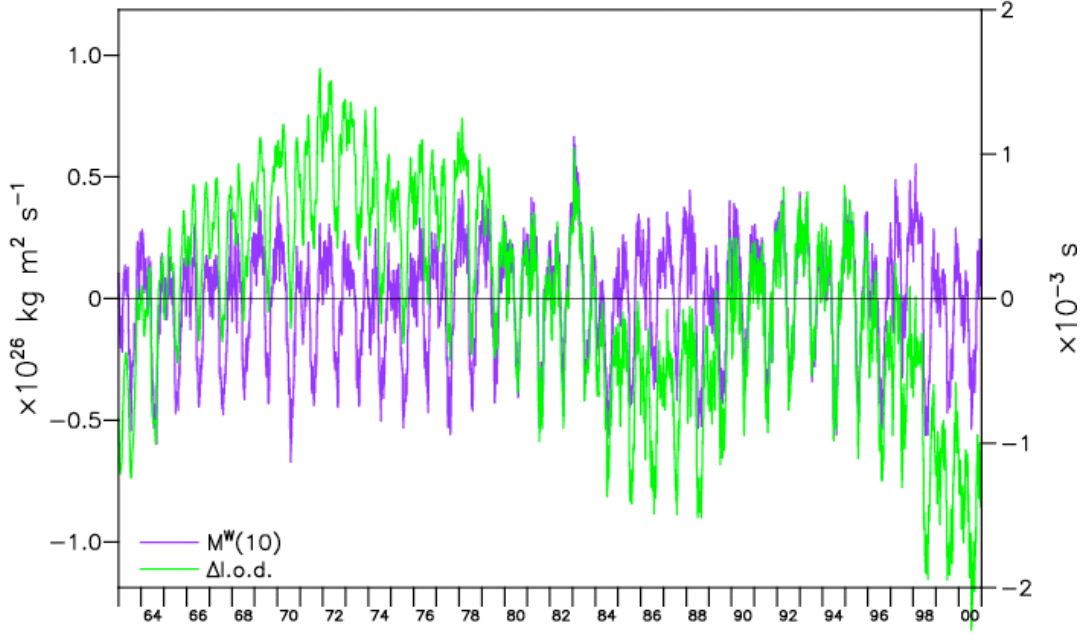
## AAM and Length of Day



Filtered

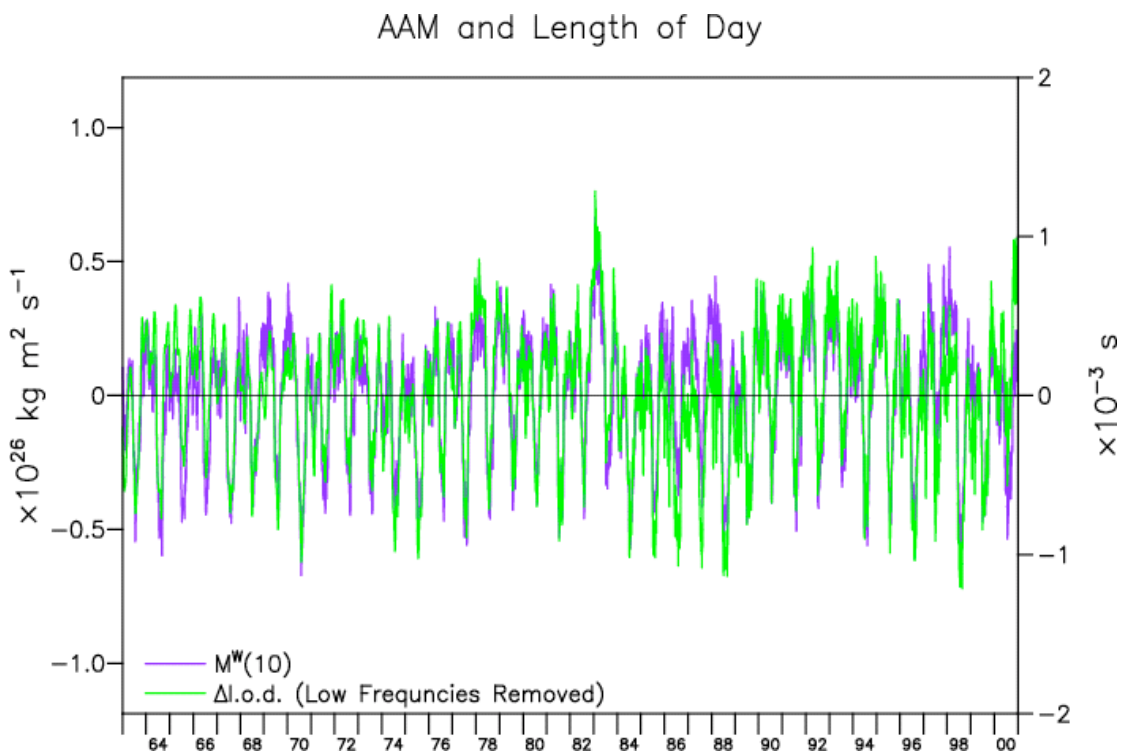
*Courtesy of David Salstein*

Raw



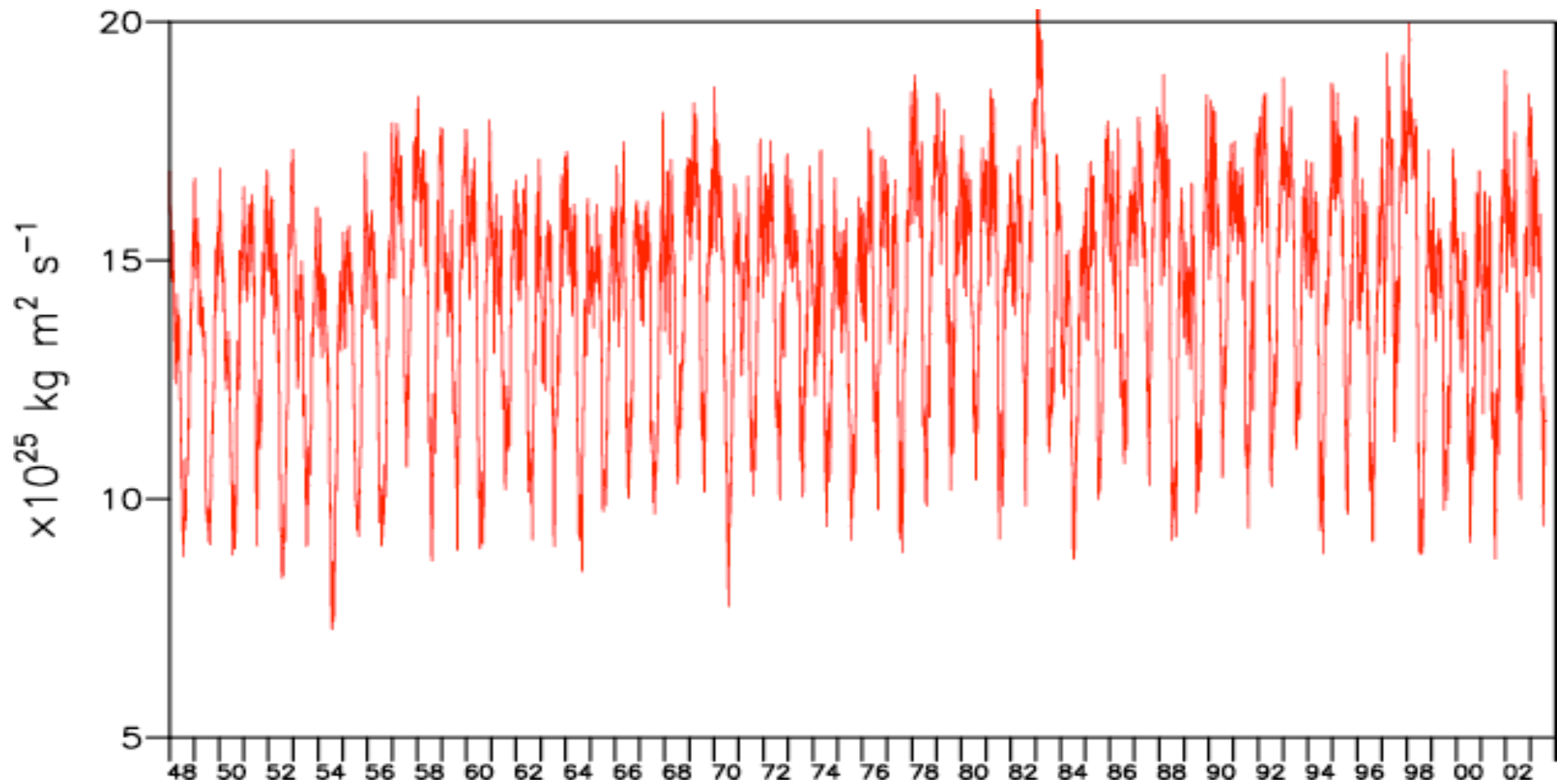
$$\Delta M = k \times \Delta(L.O.D.)$$

Filtered



Courtesy of David Salstein

## NCEP/NCAR Reanalysis AAM



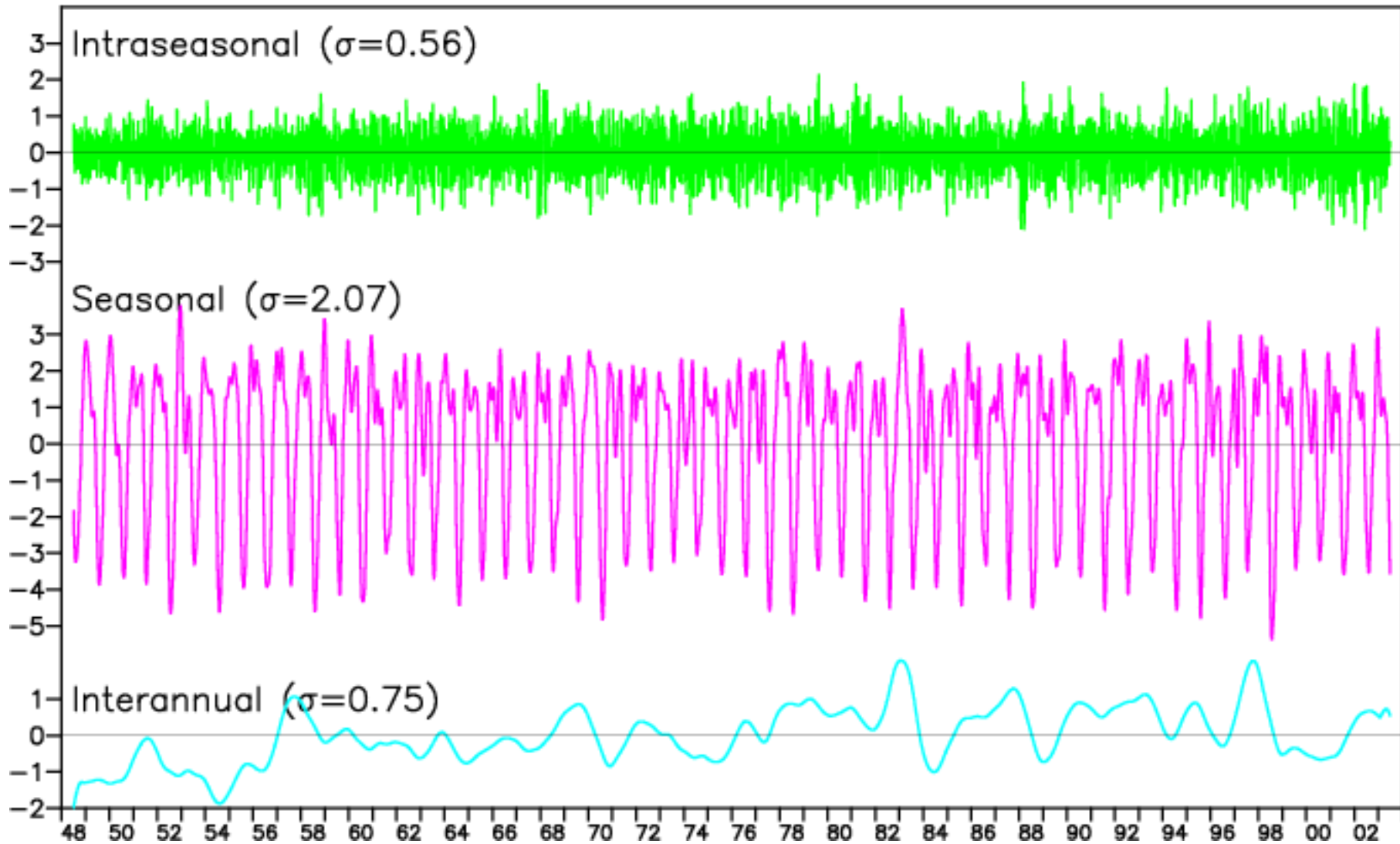
Note large seasonal cycle in angular momentum: factor of 2  
between Jan/Feb and Jul/Aug

*Courtesy of David Salstein*

# Breakdown into frequency bands

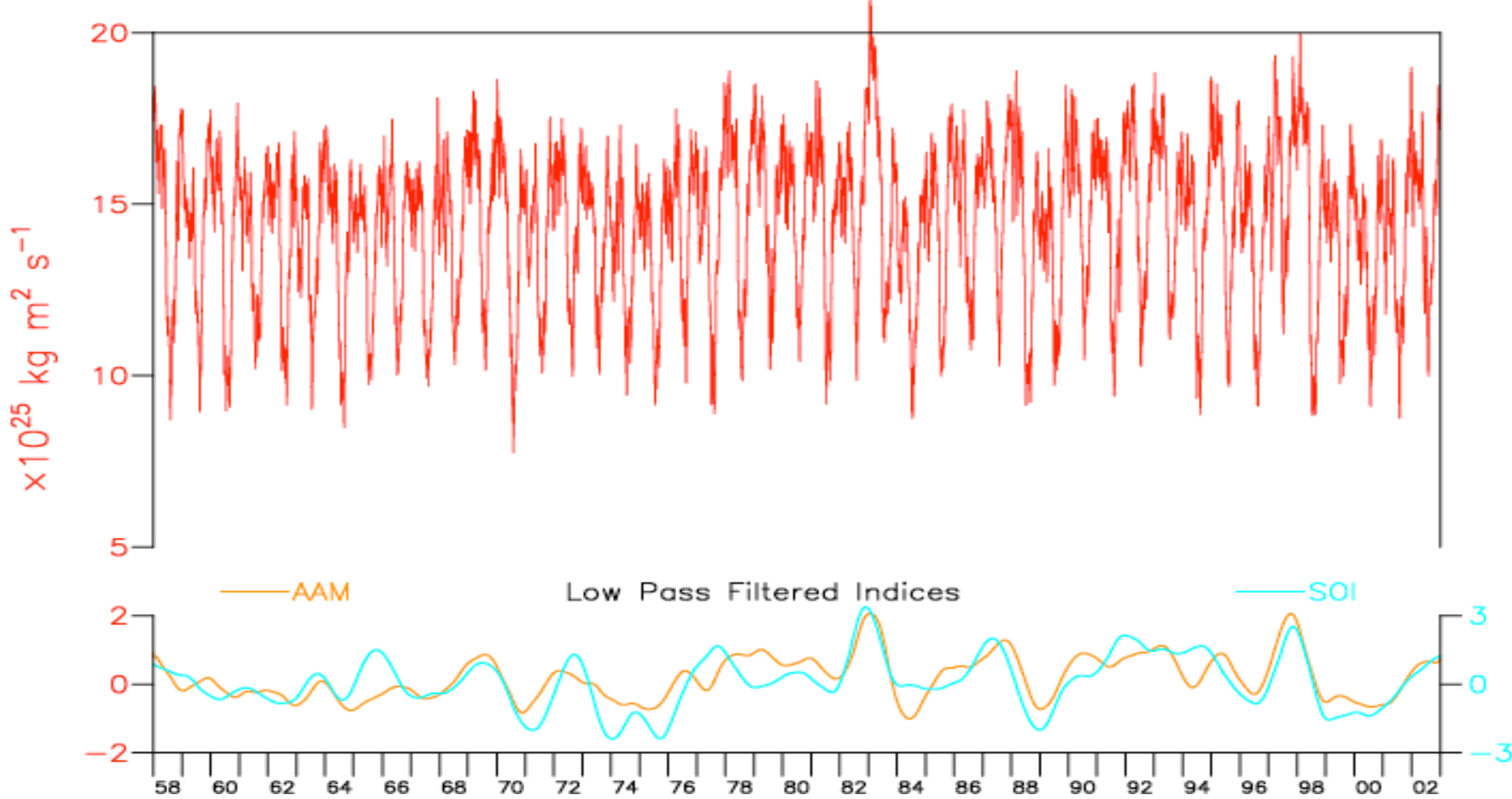
Jan. 1948–Dec. 2003

$\times 10^{25} \text{ kg m}^2 \text{ s}^{-1}$



Courtesy of David Salstein

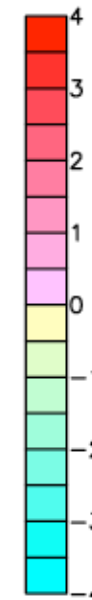
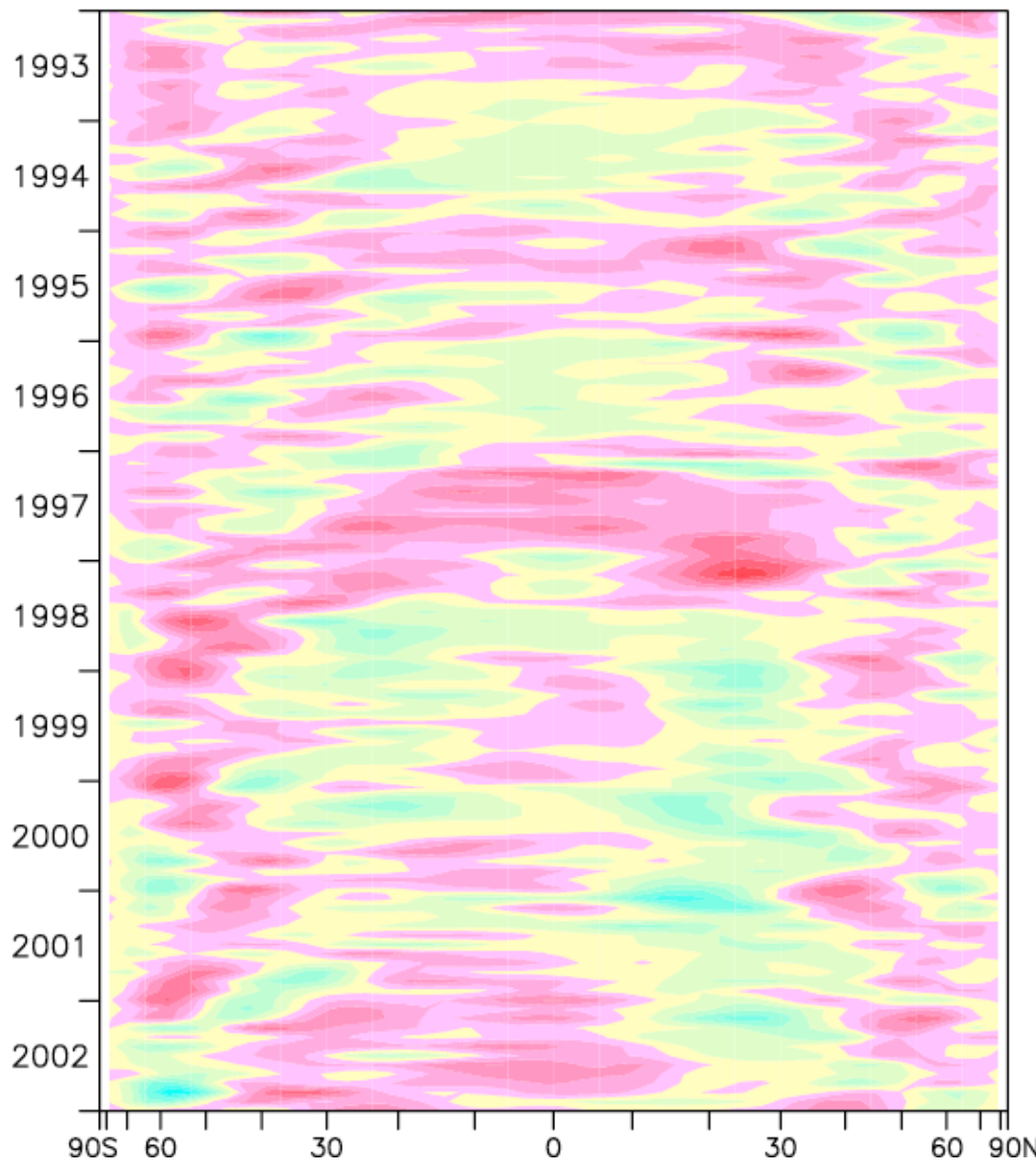
## Atmospheric Angular Momentum (AAM), 1958–2002



SOI = –Southern Oscillation Index; peaks correspond to El Nino events

*Courtesy of David Salstein*

Reanalysis Belt  $M^W(10)$  Anomaly  
( $\times 10^{24}$  kg m $^2$  s $^{-1}$ )



Positive AAM  
anomalies  
in tropics  
coincide with  
El Niño events  
(e.g., 1997-98)

*Courtesy of David Salstein*

# Mountain and friction torques

$$T_{mountain} = -R^2 \iint p_s \frac{\partial H}{\partial \lambda} \cos \phi d\phi d\lambda$$

$$T_{friction} = R^3 \iint \tau \cos^2 \phi d\phi d\lambda$$

$T_{gravity-wave}$  = Frictional related to sub-grid scale  
Action in the atmospheric model

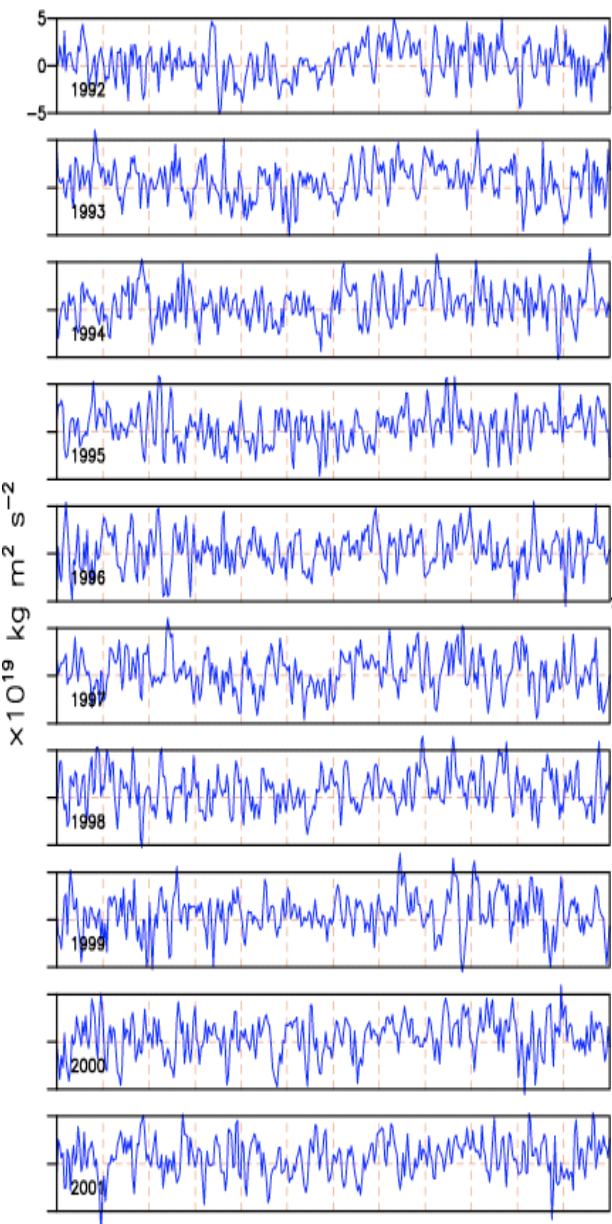
R=Earth radius,  $p_s$ =surface pressure, H=topographic height

$\tau$ =frictional stress, related to winds and roughness (model)

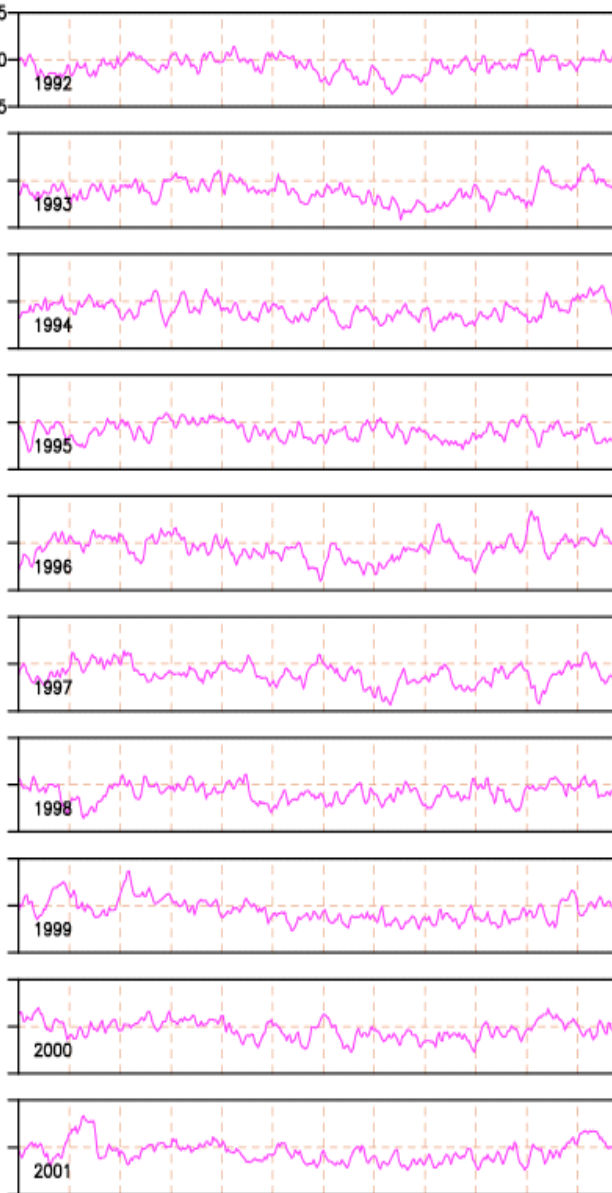
$\phi$ =longitude    $\lambda$ =latitude

*Courtesy of David Salstein*

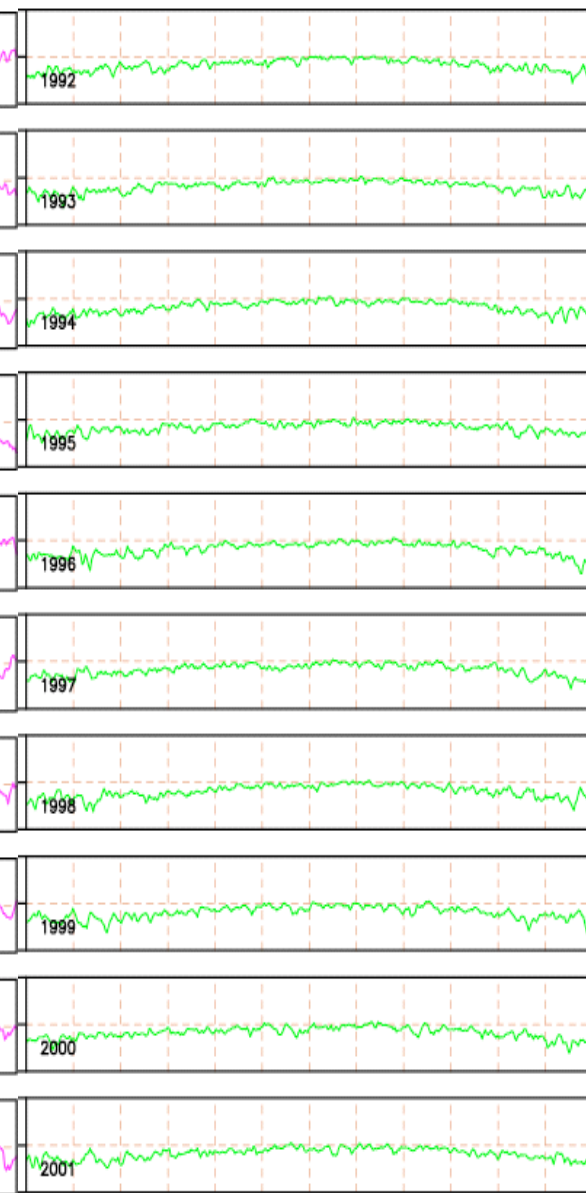
Mountain Torque



Friction Torque



Gravity Wave Torque



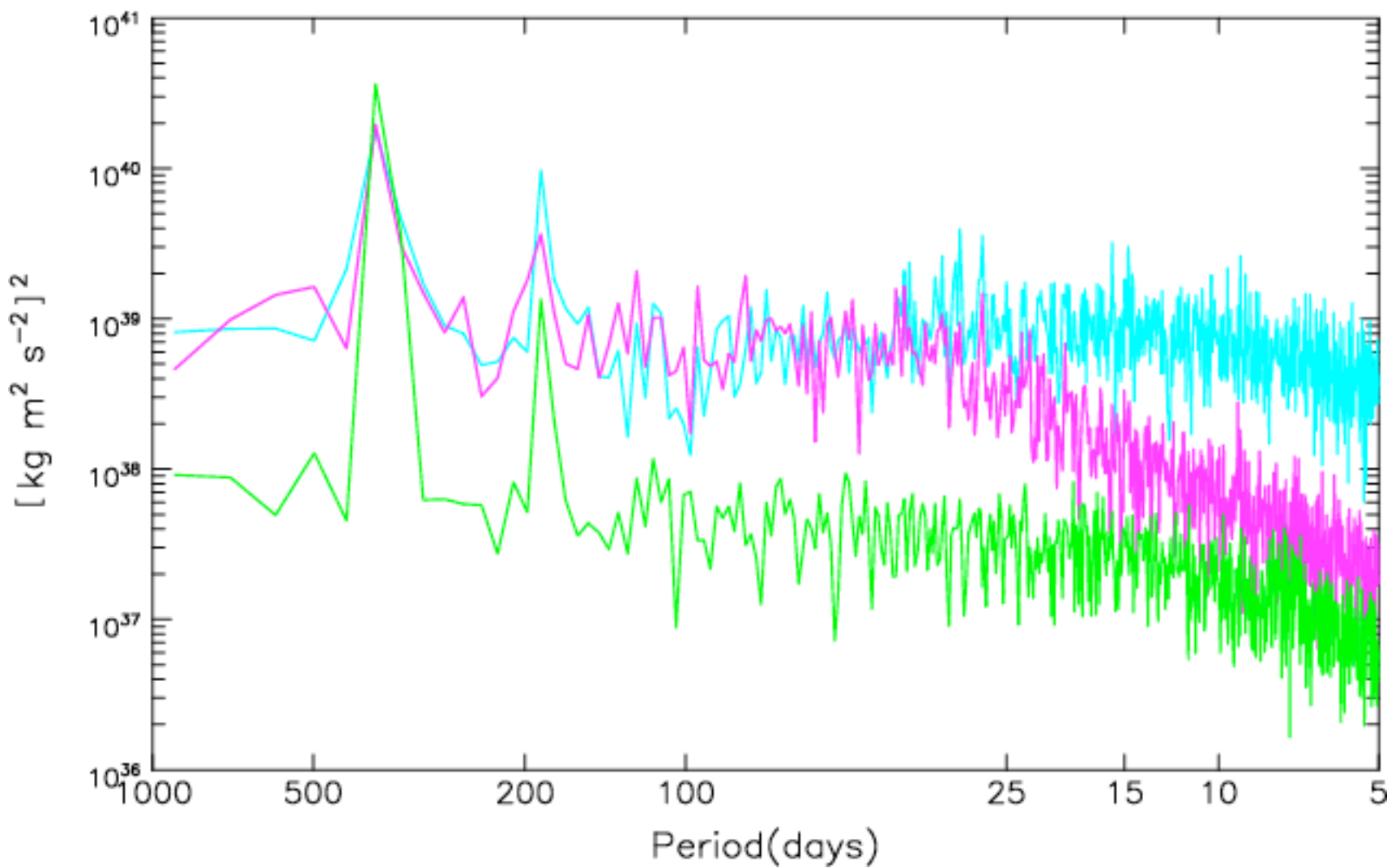
Courtesy of David Salstein

# NCEP Reanalysis Torques Power Spectra (1958–2002)

Mountain

Friction

Gravity Wave



*Courtesy of David Salstein*

# Regional Sources of Mountain Torque Variability and High-Frequency Fluctuations in Atmospheric Angular Momentum

HAIG ISKENDERIAN AND DAVID A. SALSTEIN

1682

MONTHLY WEATHER REVIEW

VOLUME 126

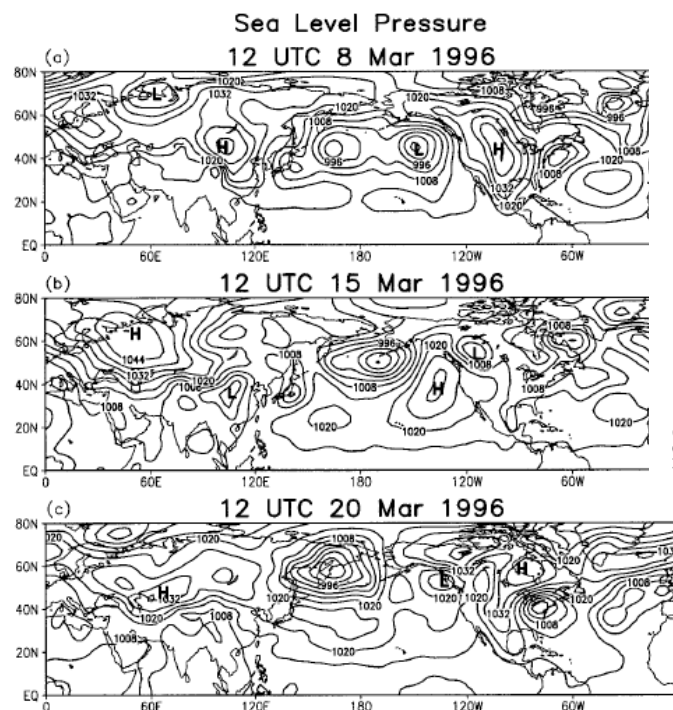
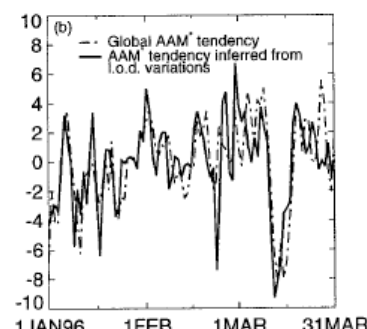
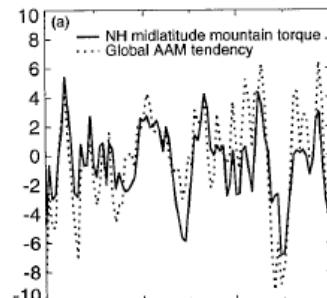
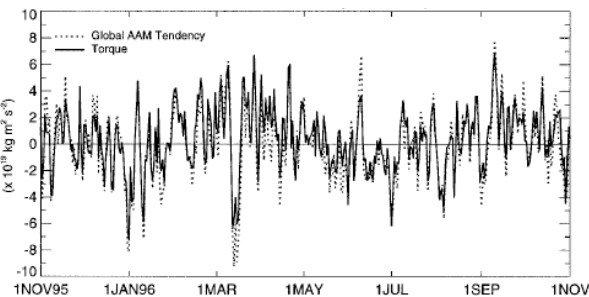


FIG. 8. Sea level pressure at 1200 UTC for (a) 8 March, (b) 15 March, and (c) 20 March 1996. Contours are every 6 hPa. Highs and lows discussed in the text are indicated by the letters H and L.

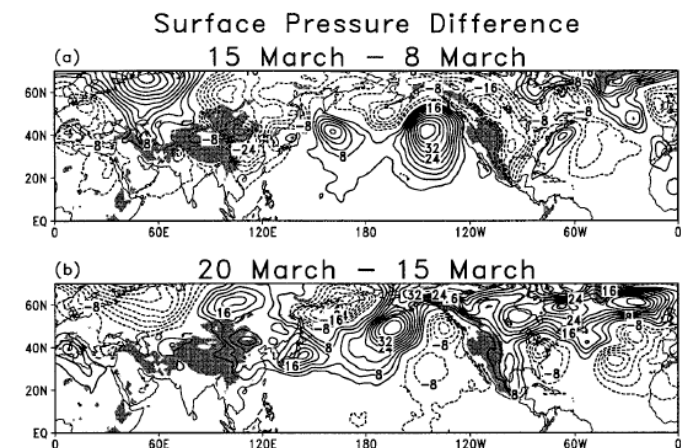
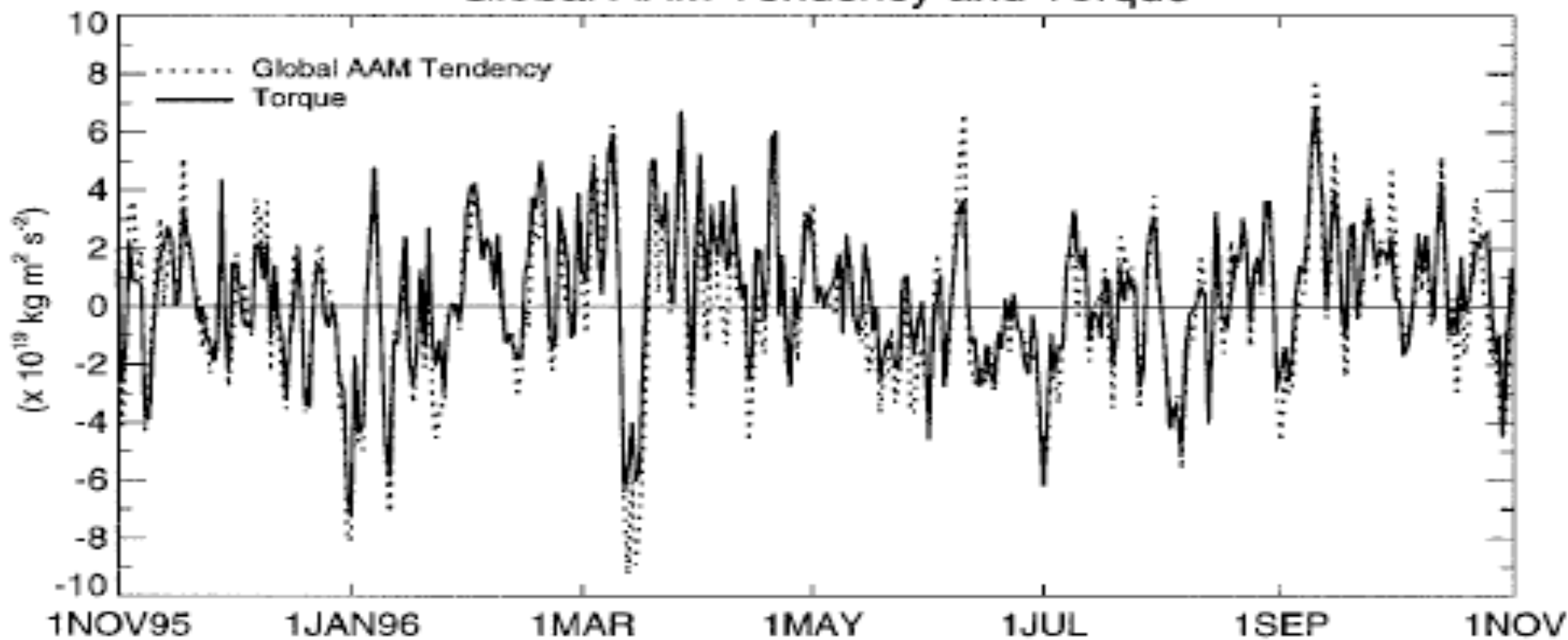
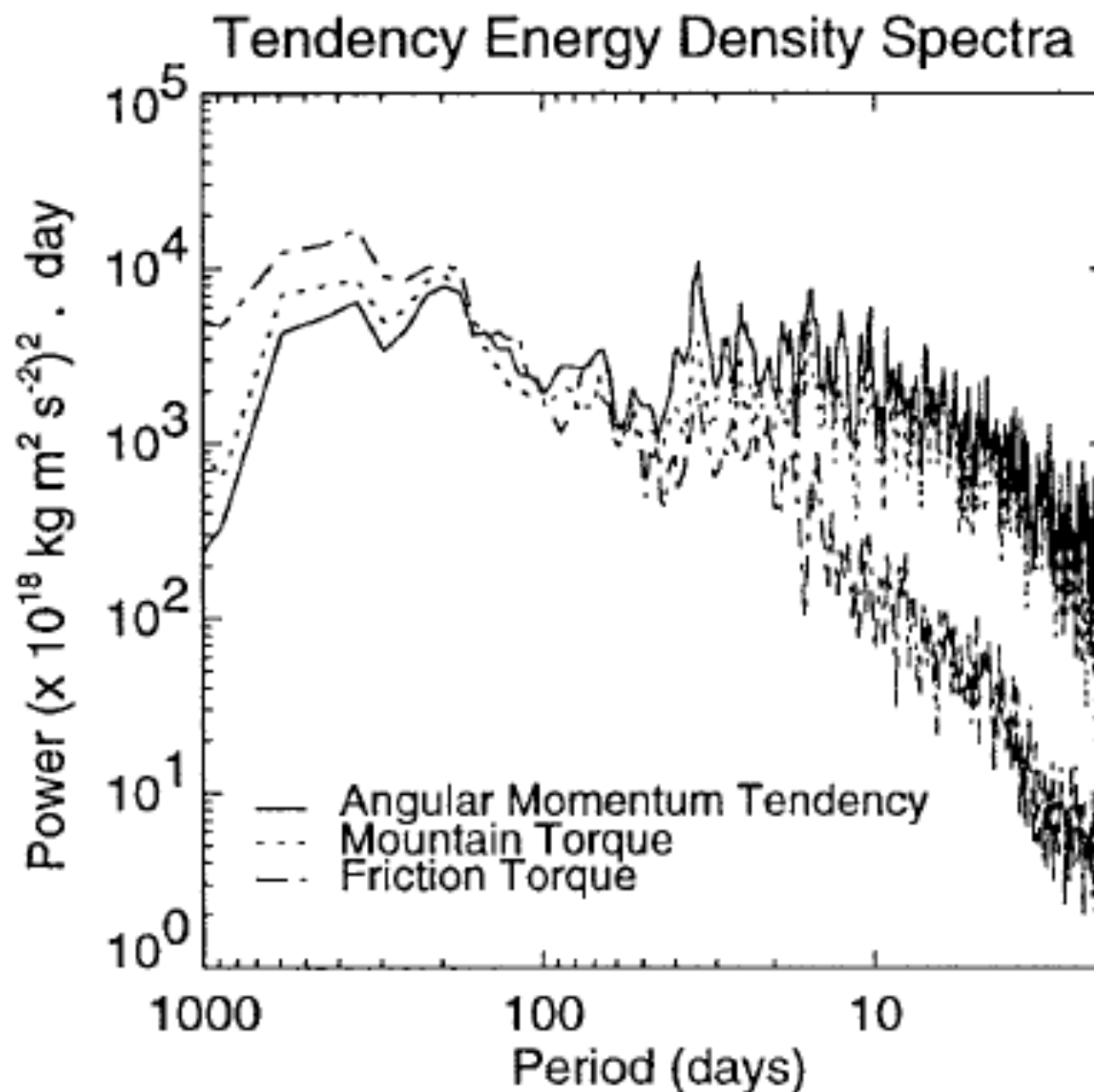


FIG. 9. (a) Difference in surface pressure between 1200 UTC 15 March and 1200 UTC 8 March 1996 (every 4 hPa contoured, zero line omitted). Positive contours are solid and negative dashed. (b) Same as (a) except between 1200 UTC 20 March and 1200 UTC 15 March. Shading indicates surface elevation of at least 1000 m.

### Global AAM Tendency and Torque



# Global Torques and AAM





600 mb

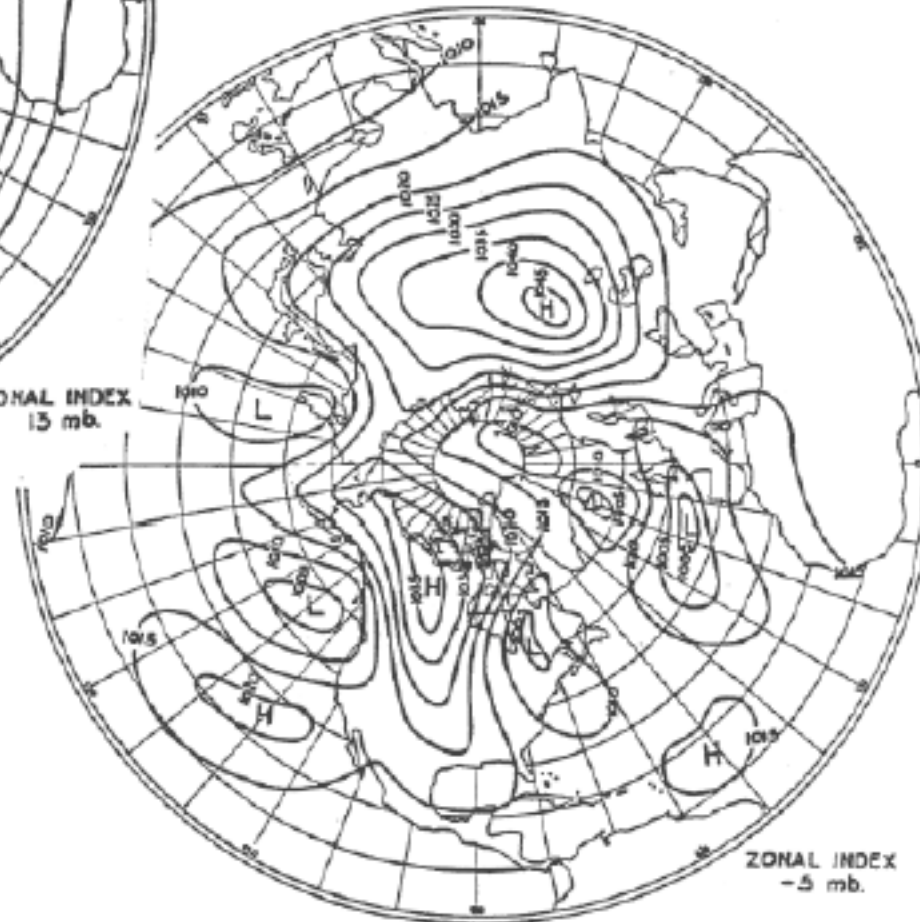
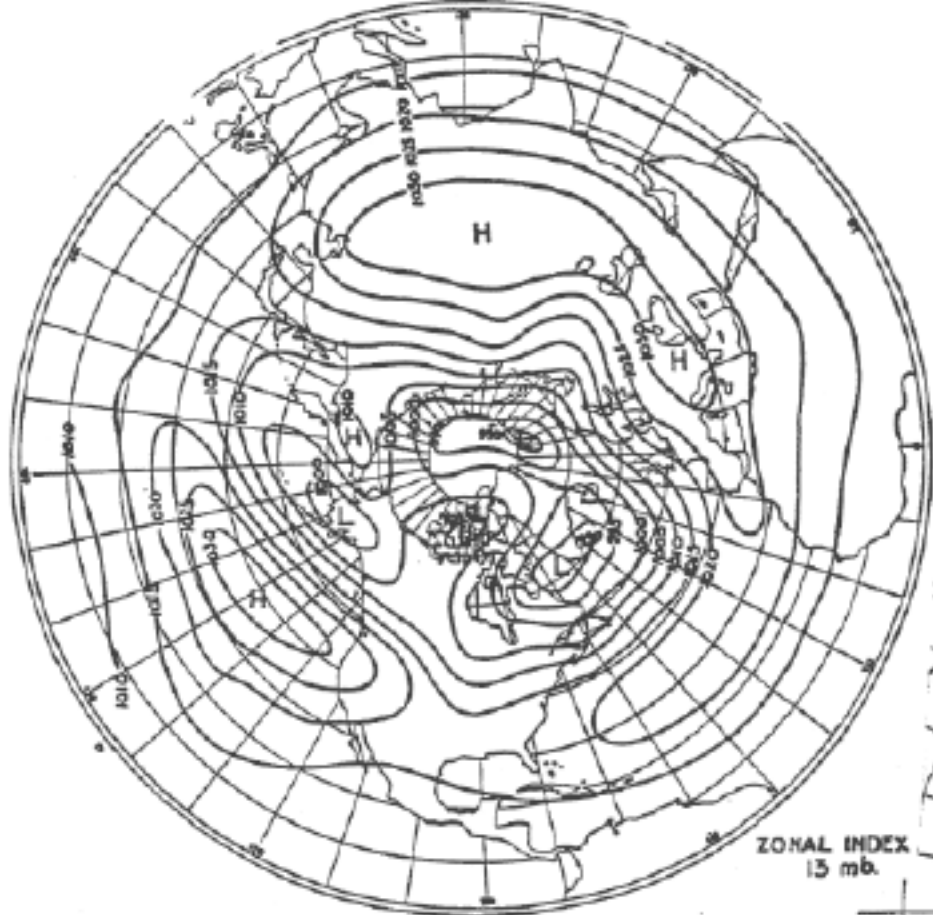
700 mb

800 mb

900 mb

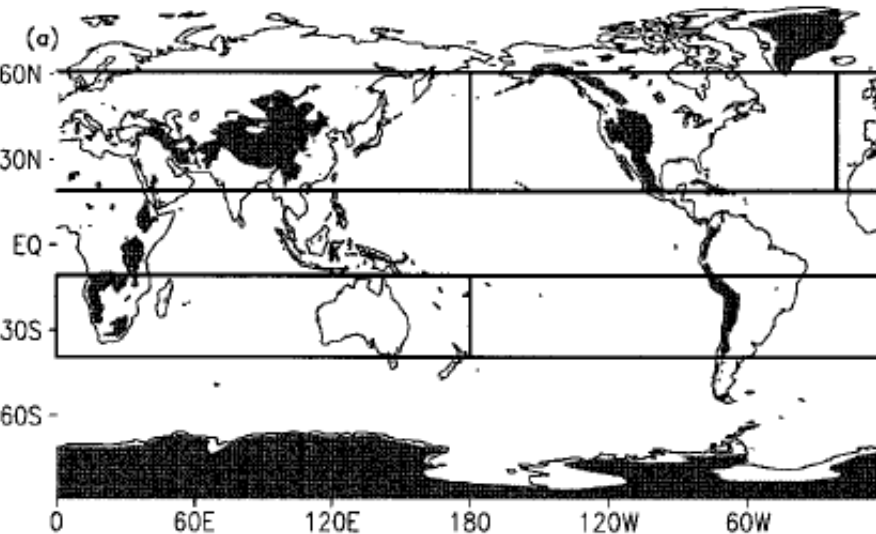
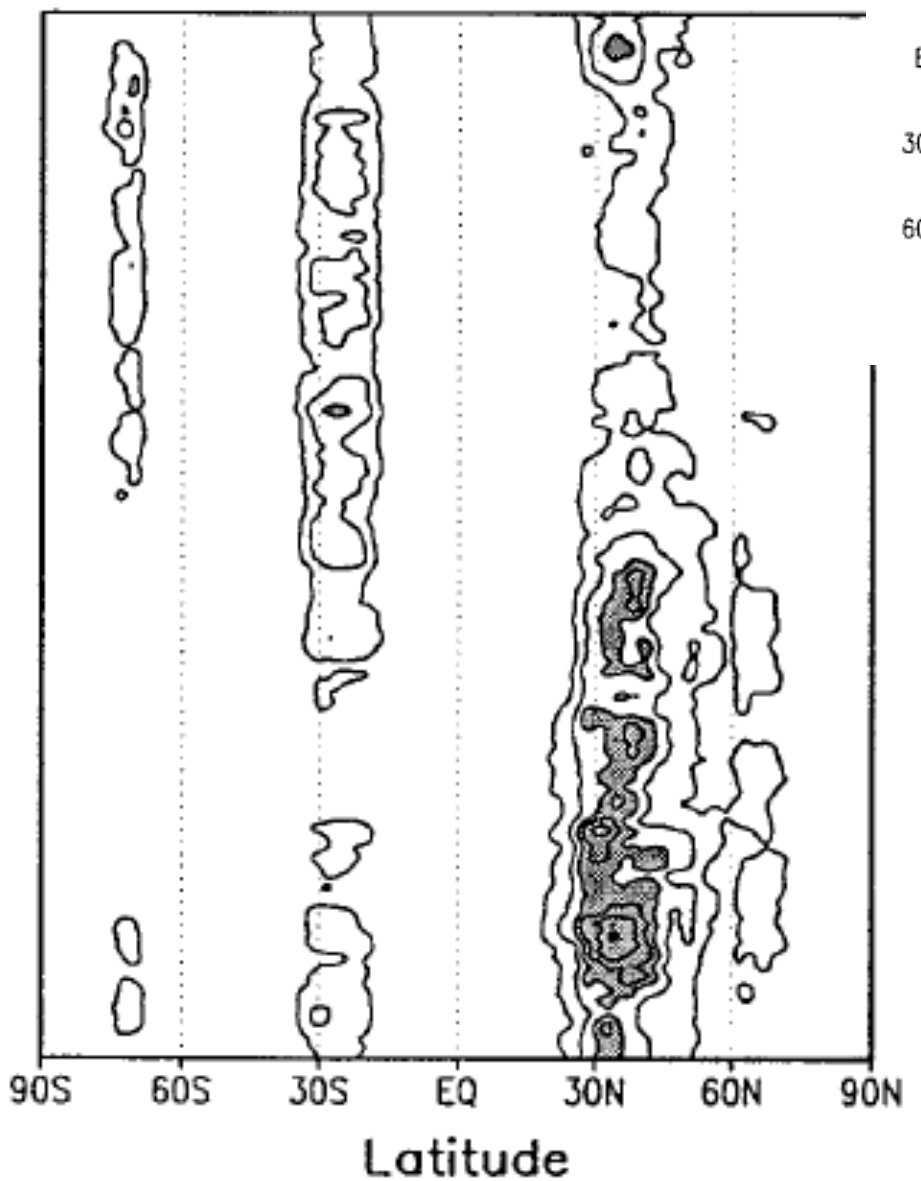
1000 mb

From Willett and Sanders



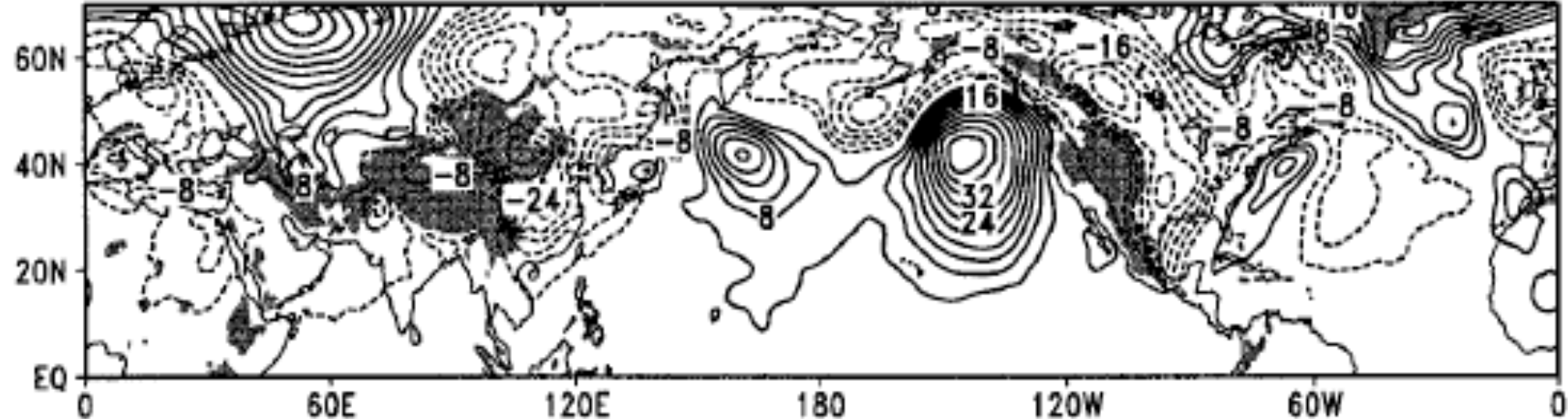
## Mountain Torque Variance (14-day moving windows)

MAY  
JUN  
JUL  
AUG  
SEP  
OCT  
NOV  
DEC  
JAN  
FEB  
MAR  
APR



# Surface Pressure Difference

## 15 March – 8 March



## 20 March – 15 March

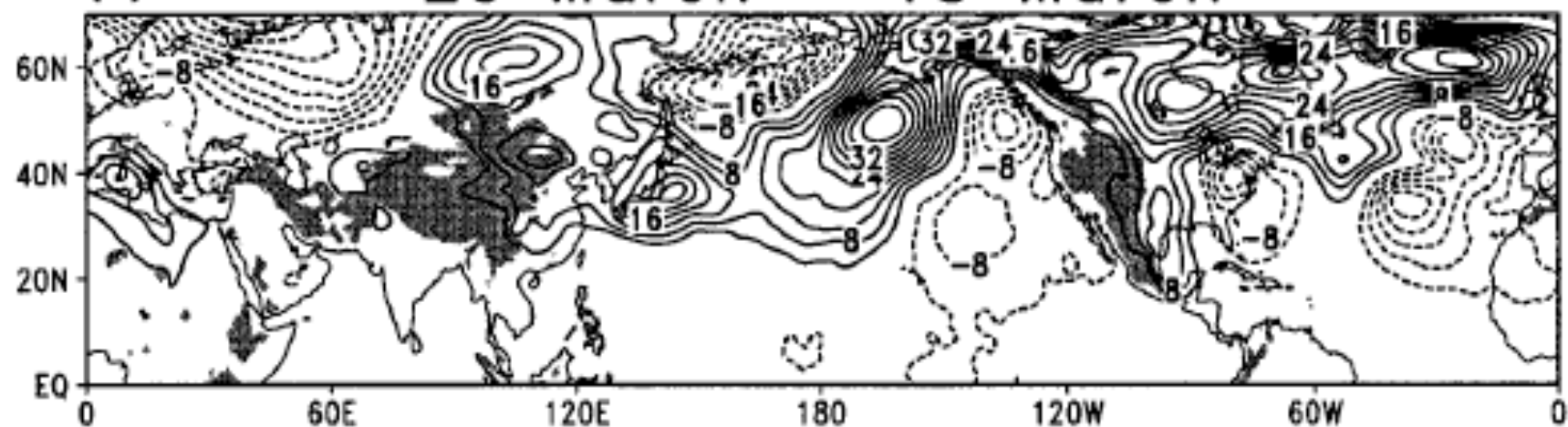
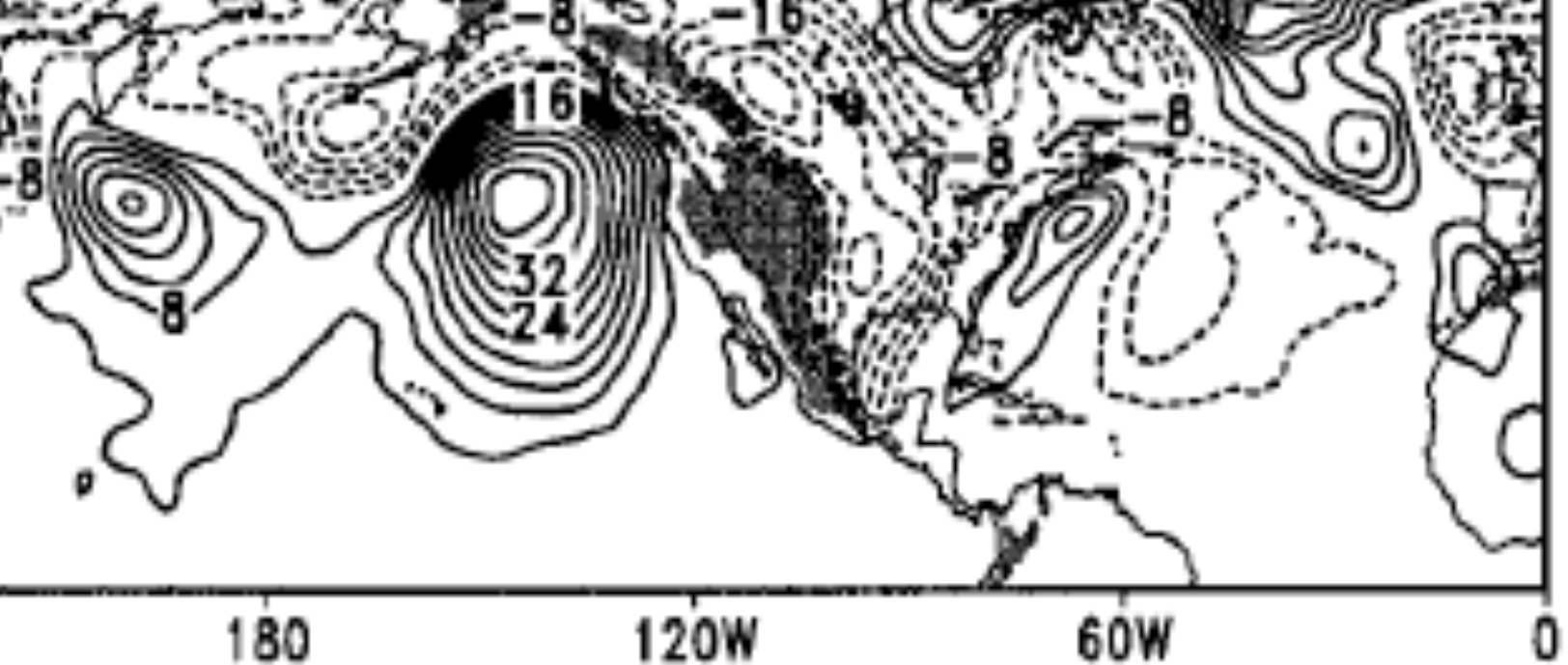
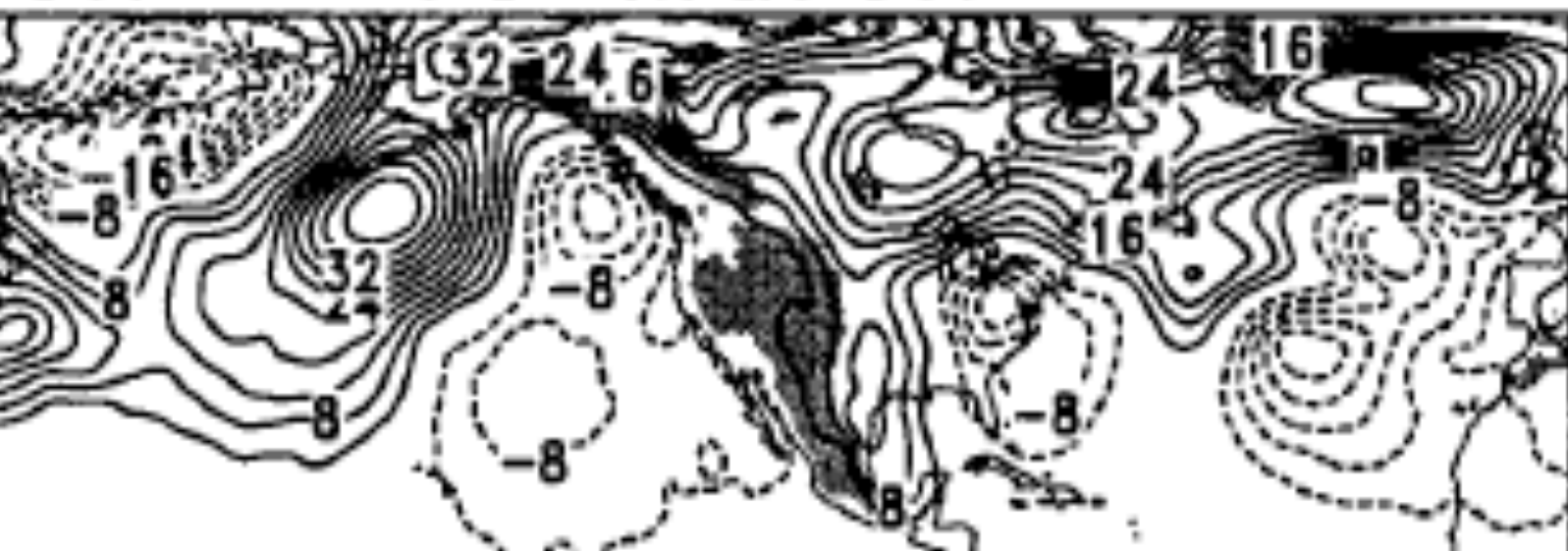


FIG. 9. (a) Difference in surface pressure between 1200 UTC 15 March and 1200 UTC 8 March 1996 (every 4 hPa contoured, zero line omitted). Positive contours are solid and negative dashed. (b) Same as (a) except between 1200 UTC 20 March and 1200 UTC 15 March. Shading indicates surface elevation of at least 1000 m.



March – 15 March



For steady state:

Integrated over the globe

Net torque on atmosphere = 0

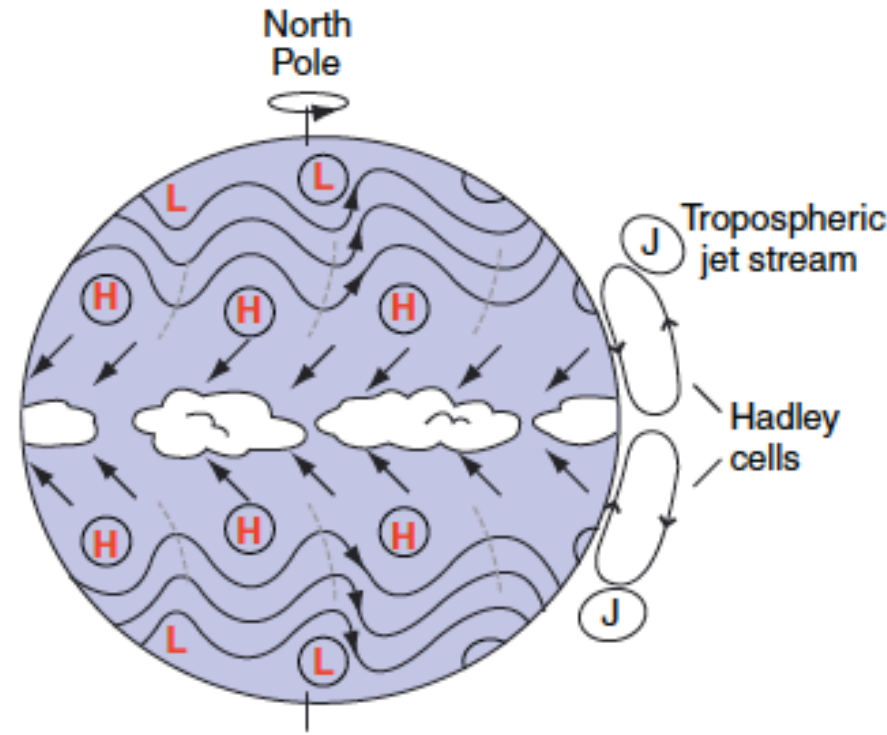
In the absence of mountains  
net frictional torque = 0

if the surface winds are nonzero, there must be regions  
of easterlies and westerlies

For steady state:

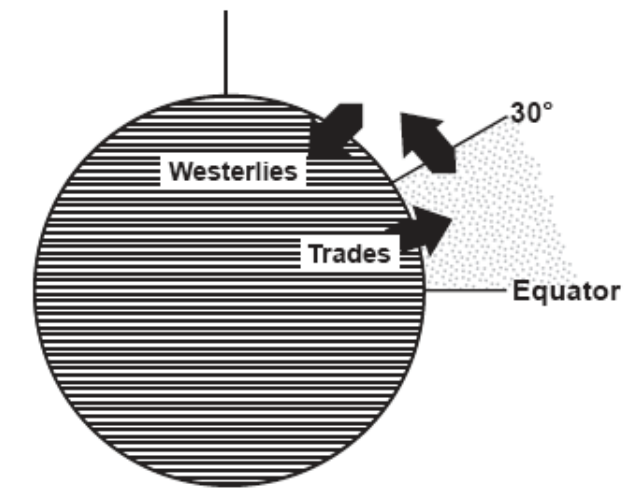
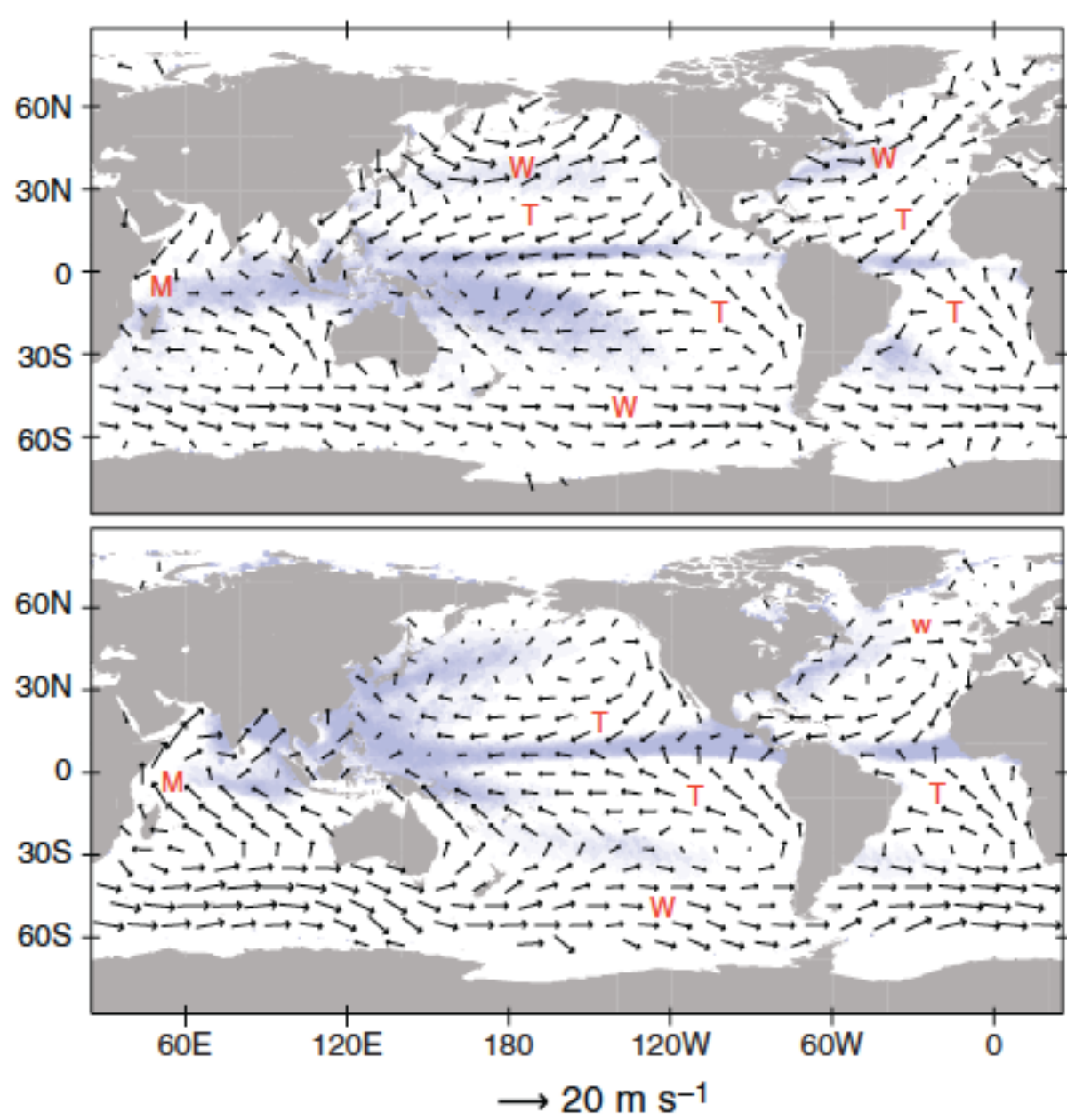
Integrated over the globe

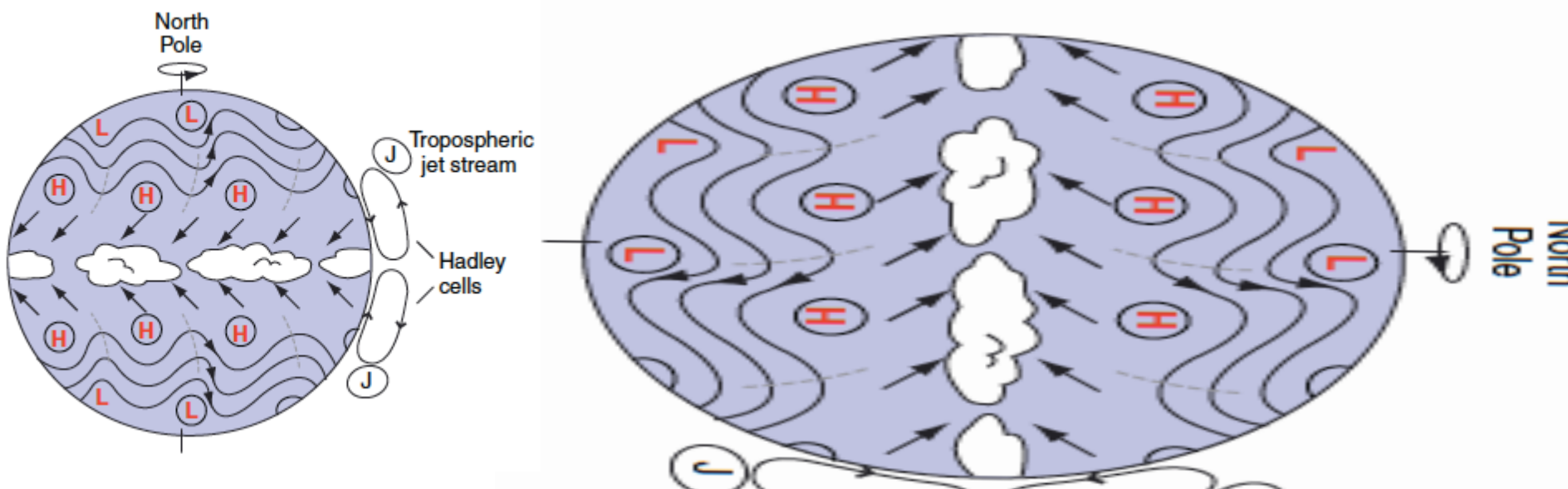
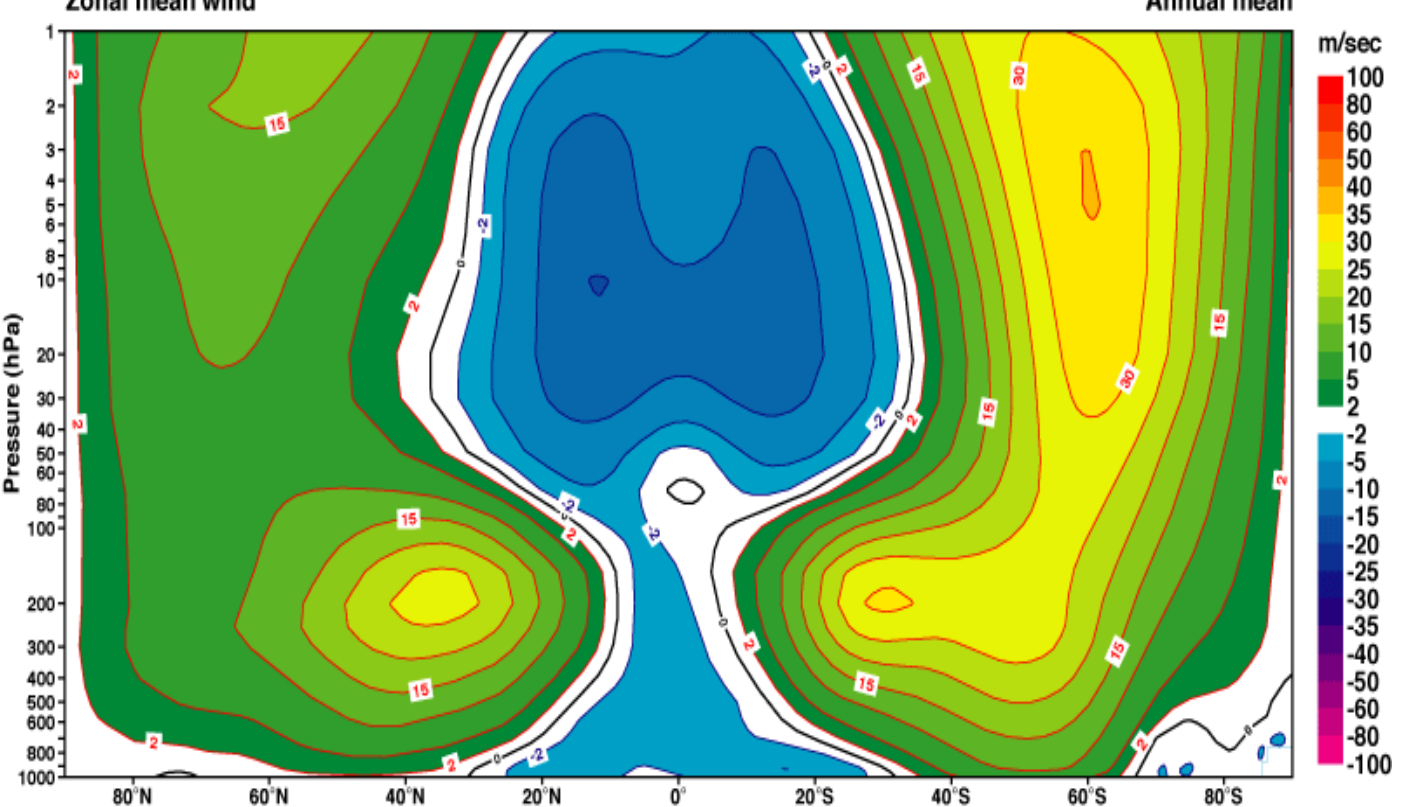
Net torque on atmosphere = 0

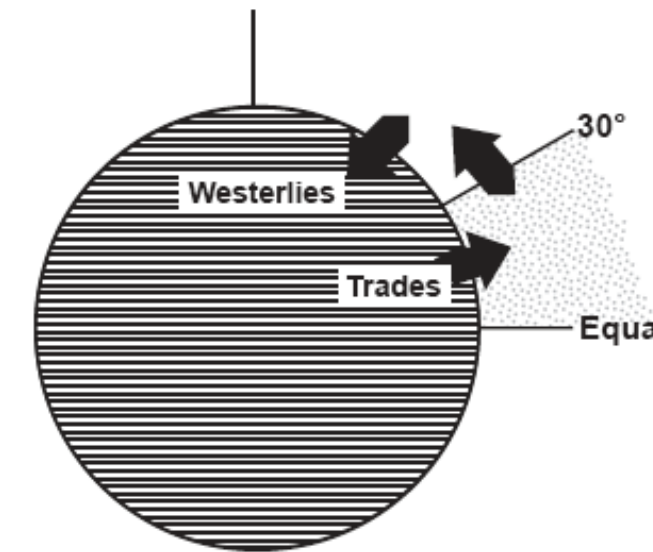
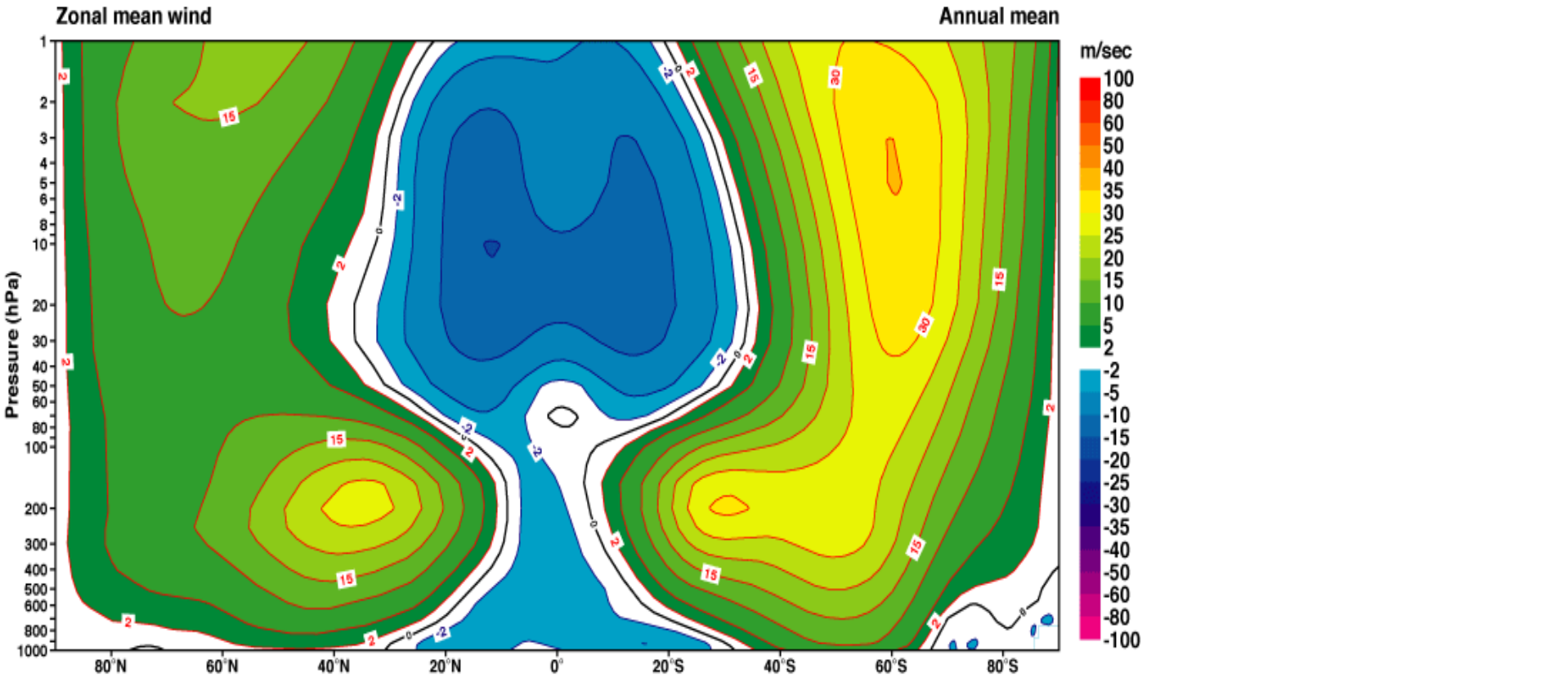


In the absence of mountains  
net frictional torque = 0

if the surface winds are nonzero, there must be regions  
of easterlies and westerlies

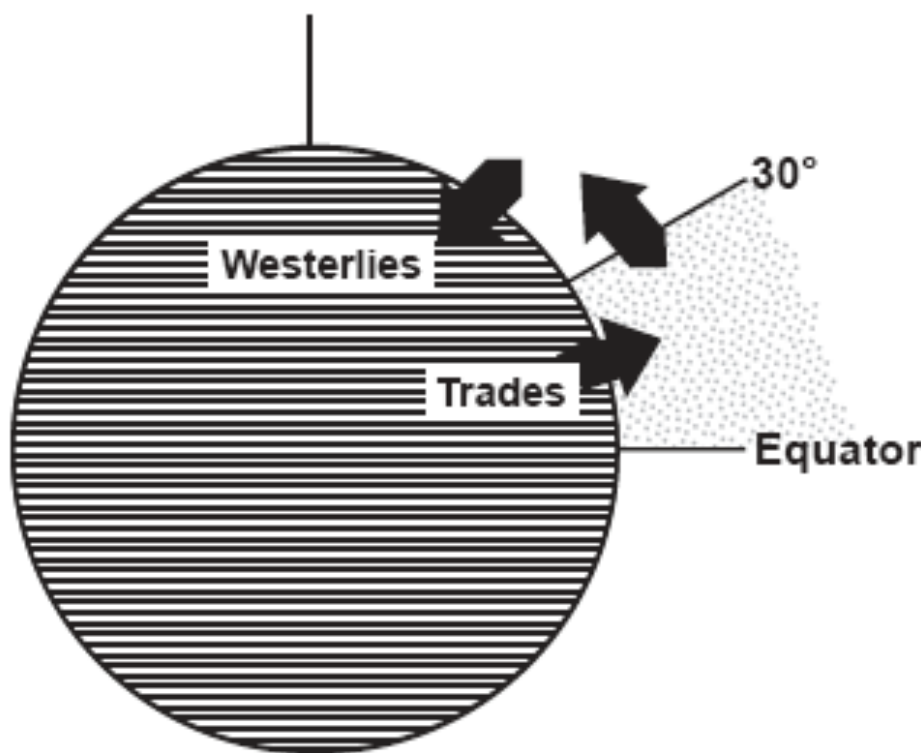






$$-2\pi R_E^3 \int_{eq}^{30^\circ} [\bar{\tau}_x] \cos^2 \phi d\phi = \frac{2\pi R_E \cos \phi}{g} \int_{30^\circ} [\bar{m}v] dp$$

Torque equatorward of  $30^\circ$  = Transport across  $30^\circ$



Another balance requirement:

$$-2\pi R_E^3 \int_{eq}^{30^\circ} [\bar{\tau}_x] \cos^2 \phi d\phi = \frac{2\pi R_E \cos \phi}{g} \int_{30^\circ} [\bar{mv}] dp$$

Torque equatorward of  $30^\circ$  = Transport across  $30^\circ$

**It follows that there must be a poleward flux of AAM across  $30^\circ$  latitude in both hemispheres**

$$\frac{2\pi R_E \cos \phi}{g} \int_{30^\circ} [\overline{mv}] dp = \frac{2\pi \Omega R_E^3 \cos^3 \phi}{g} \int_{30^\circ} [\overline{v}] dx dp + \frac{2\pi R_E^2 \cos^2 \phi}{g} \int_{30^\circ} [\overline{uv}] dx dp$$

*Total*

$M_\Omega$

$M_r$

*requires  
poleward  
mass flux*

## Decomposition of $M_r$

$$[\bar{u}\bar{v}] = [\bar{u}] [\bar{v}] + \overline{[u]' [v]'} + [\bar{u}^* \bar{v}^*] + \left[ \overline{u^{*' } v^{*' }} \right]$$

Steady  
MMC

transient  
MMC

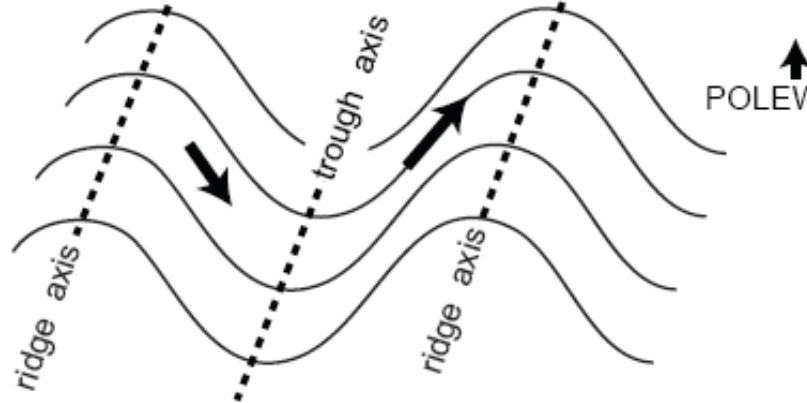
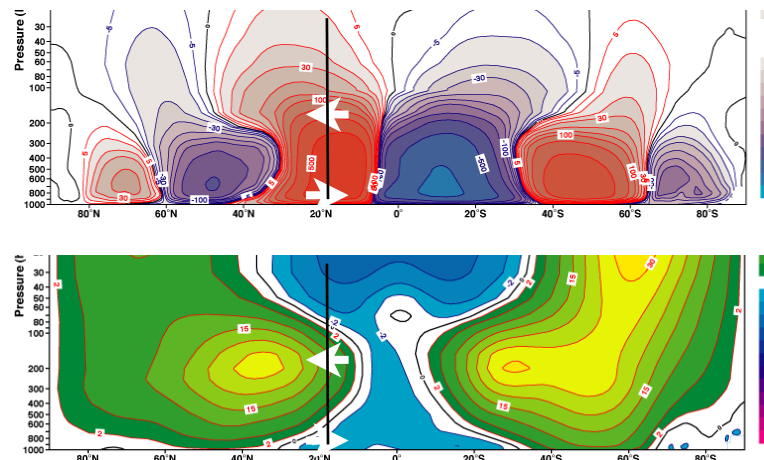
steady  
eddy

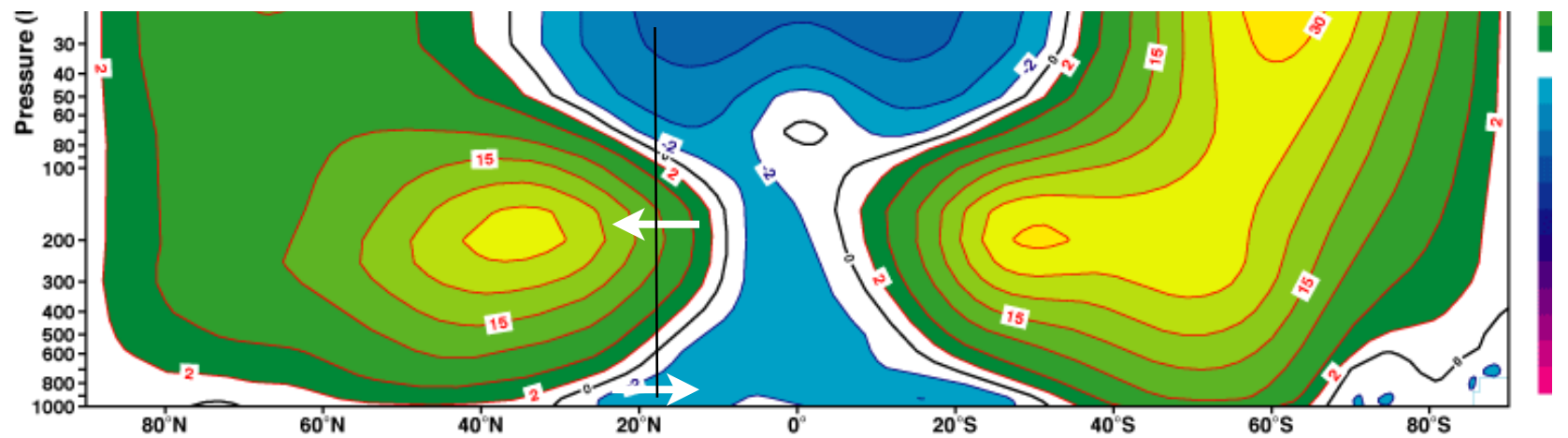
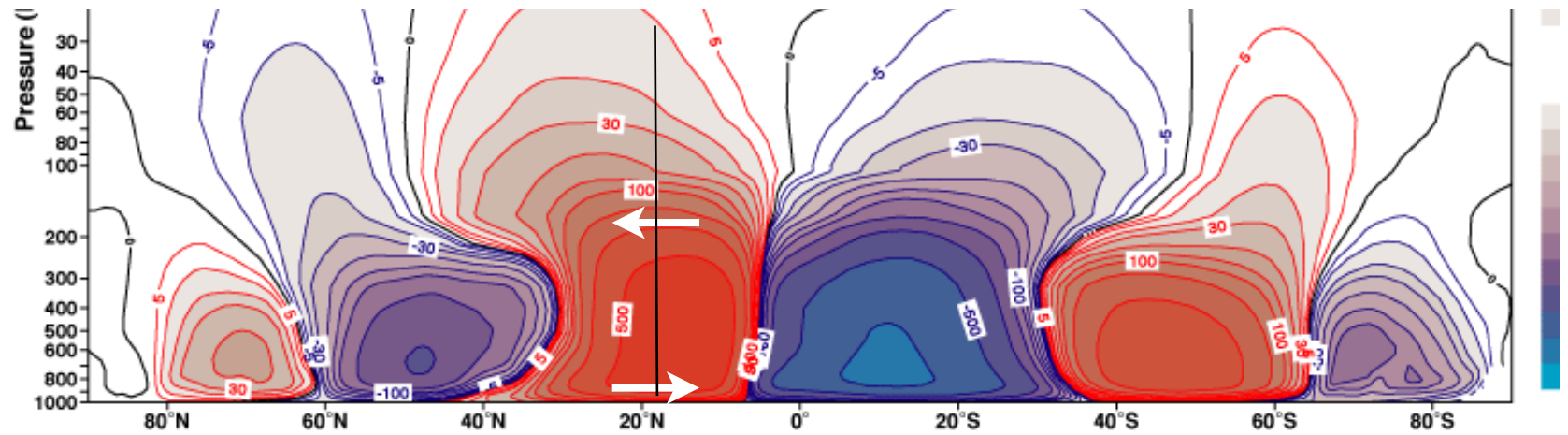
transient  
eddy

a.k.a.  
*stationary wave*

# Decomposition of $M_r$

$$[\bar{uv}] = [\bar{u}] [\bar{v}] + \overline{[u]'} [v]' + [\bar{u}^* \bar{v}^*] + \overline{[u^*'] [v^*']}$$

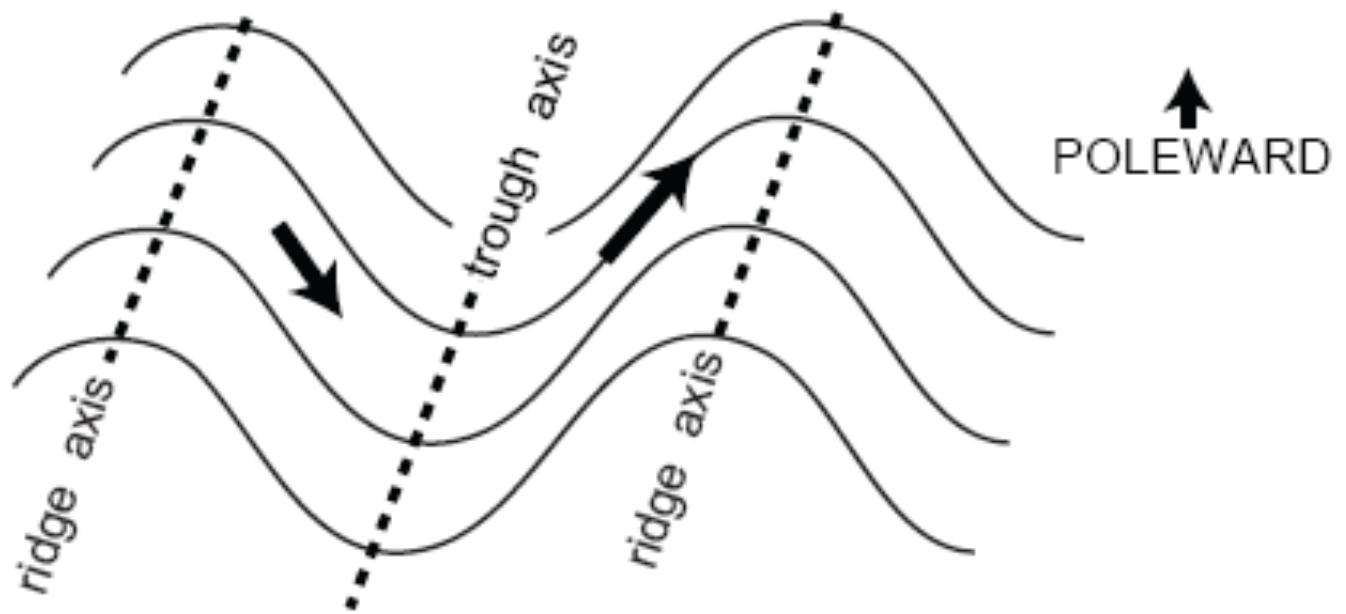




$$\int_0^{p_0} [u][v] dp$$

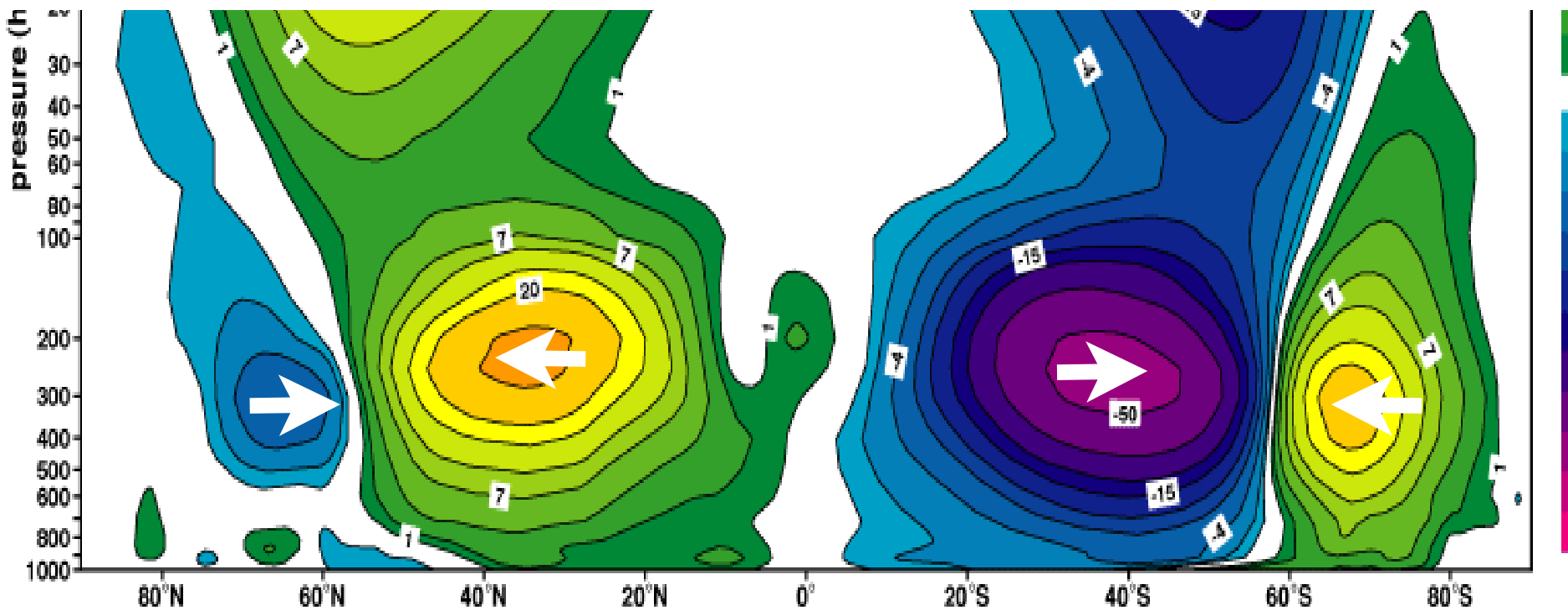
# Product Moment Formula

$$[u * v *] = r(u, v) \times \sigma_u \times \sigma_v$$

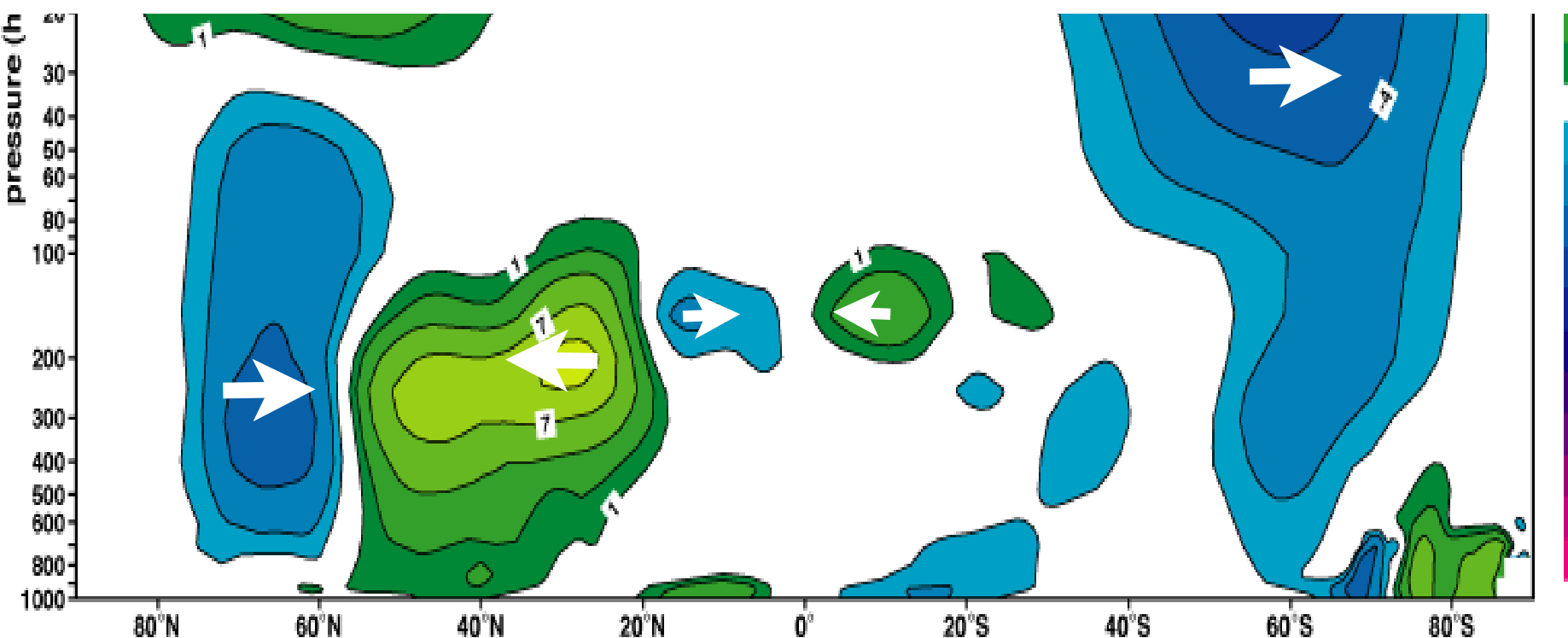


$$[u^* v^*]$$

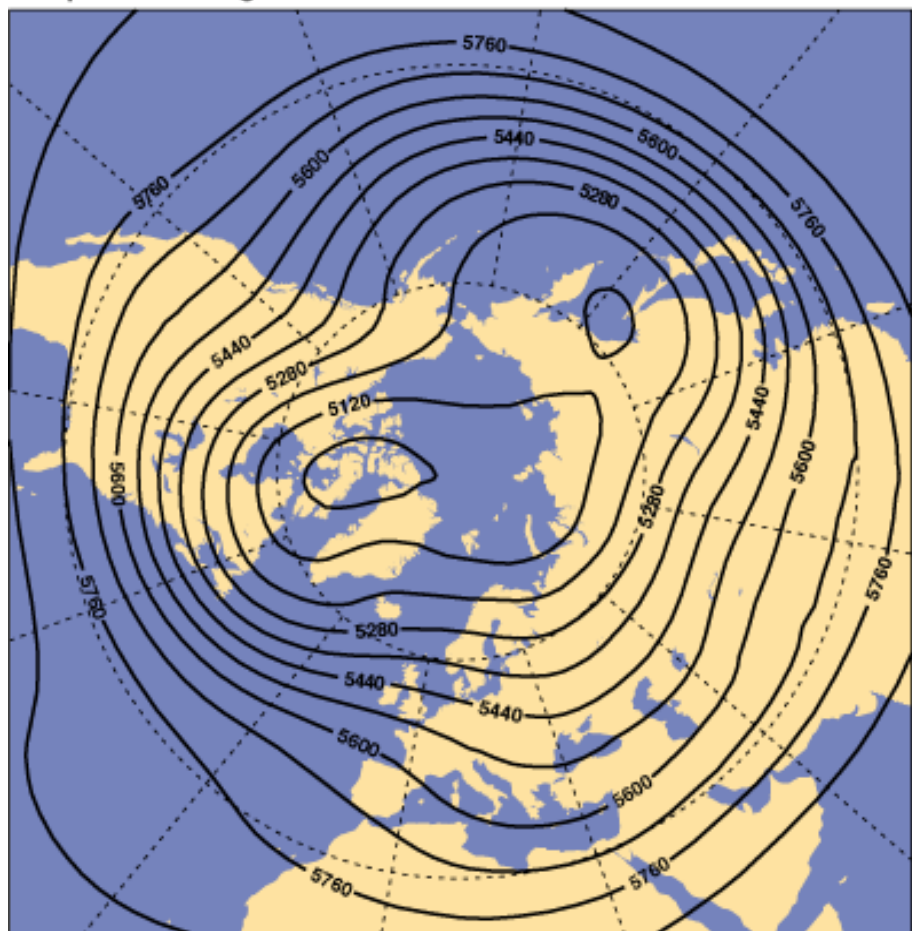
transient eddy component annual mean



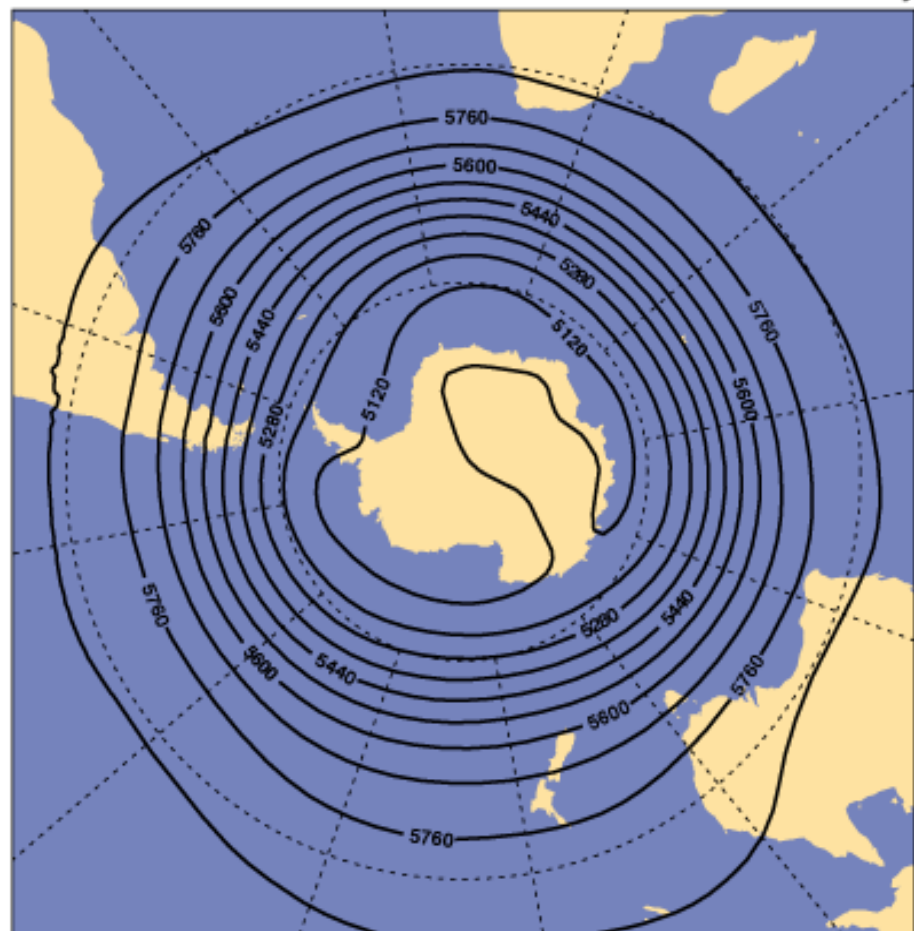
# stationary wave component annual mean

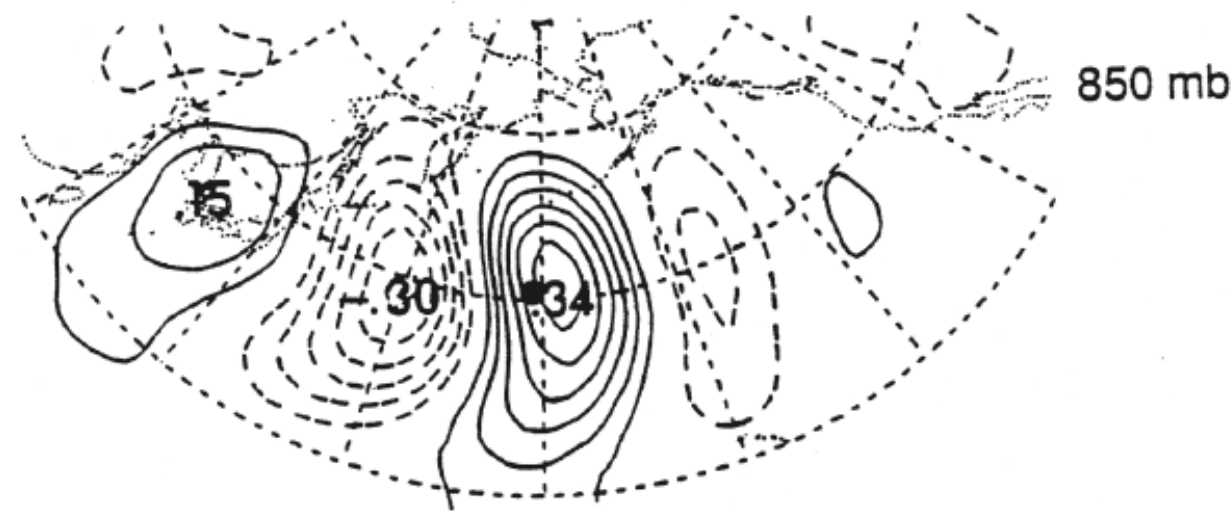
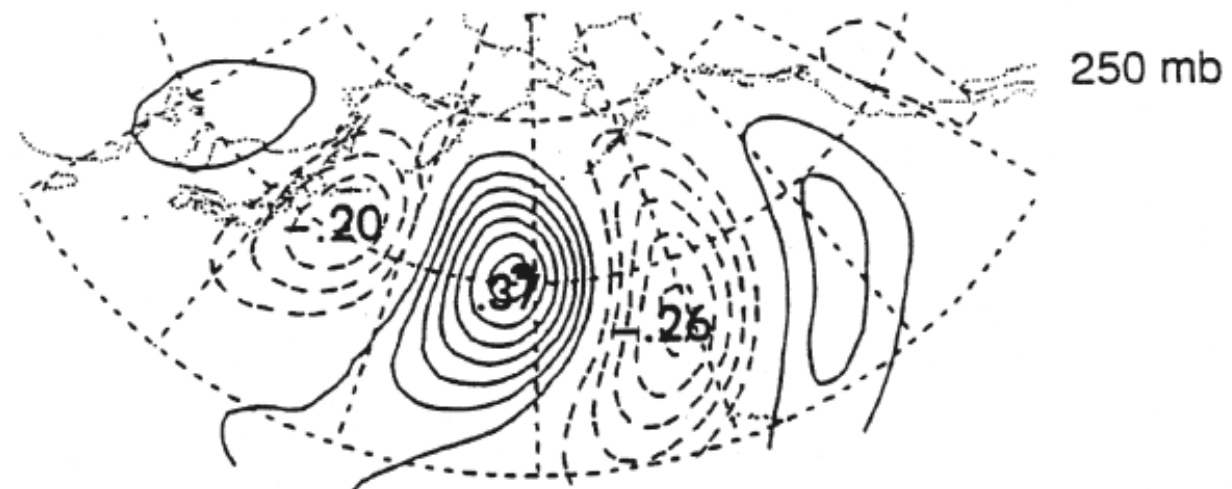


Geopotential height at 500 hPa



December-February





one-point correlation maps; 500 hPa height; highpass filtered

# Conclusions

In accordance with the balance requirements, there is a strong poleward flux of angular momentum across  $30^\circ$  latitude

The flux is greater during winter when the surface westerlies are stronger

The poleward flux across  $30^\circ$  is accomplished **exclusively by the eddies**

Transient eddies and stationary waves both contribute

Nearly all the flux occurs around the jet stream level (above 500 hPa)

**Balance requirement for an upward flux of M equatorward of  $30^\circ$  and a downward flux poleward of  $30^\circ$**

## Vertical transport of angular momentum

$$\frac{2\pi\Omega R_E^3}{g} \int - [\bar{\omega}] \cos^3 \phi dy + \frac{2\pi R_E^2}{g} \int - [\bar{u}\bar{\omega}] \cos^2 \phi dy$$

$M_\Omega$

$M_r$

$$\frac{2\pi R_E^2}{g} \int - [\bar{\omega}] (\Omega R_E \cos \phi + [\bar{u}]) \cos^2 \phi dy + \frac{2\pi R_E^2}{g} \int [\bar{u}^* \bar{\omega}^*] \cos^2 \phi dp$$

MMC term

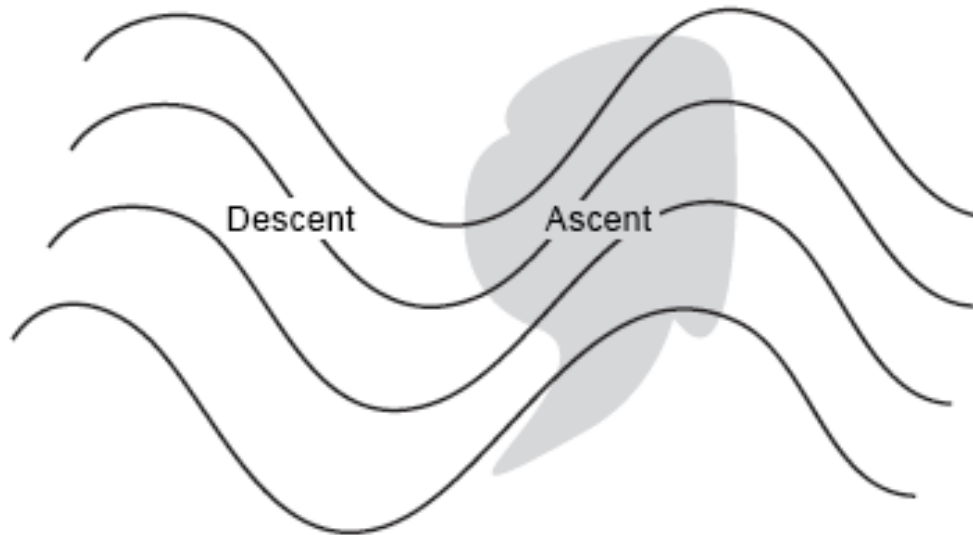
eddy term

The eddies are not the answer

Scaling arguments: extratropical eddy fluxes are too small by a factor of  $Ro$

Tropical eddy fluxes are almost nonexistent

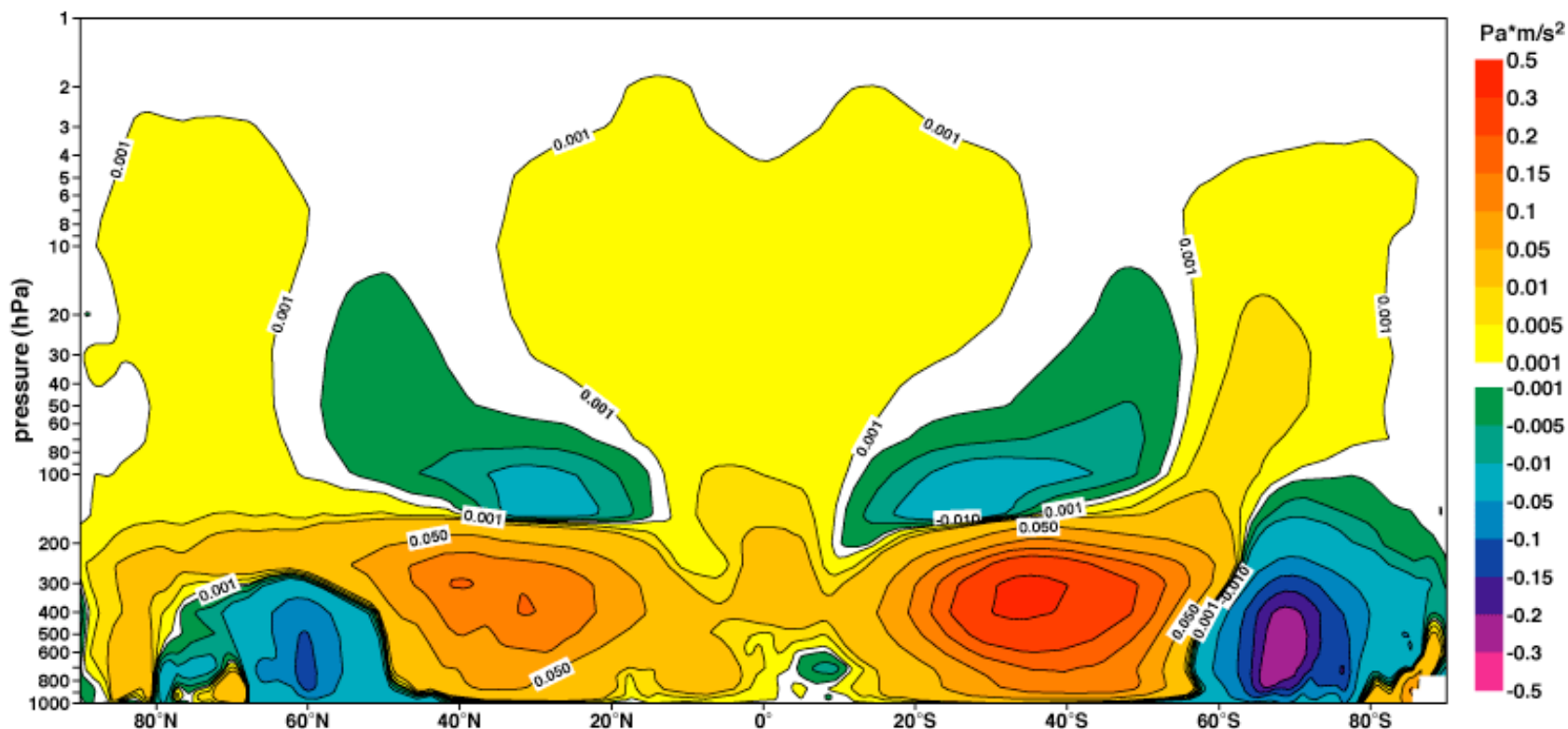
Extratropical eddy fluxes are upward; not downward



So it must be the MMC

Transient upward eddy flux of westerly wind

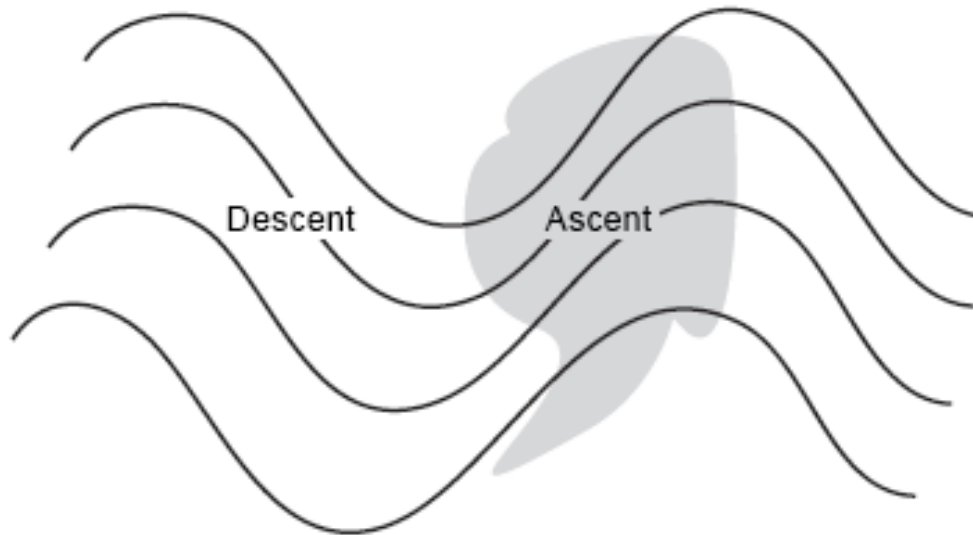
Annual mean



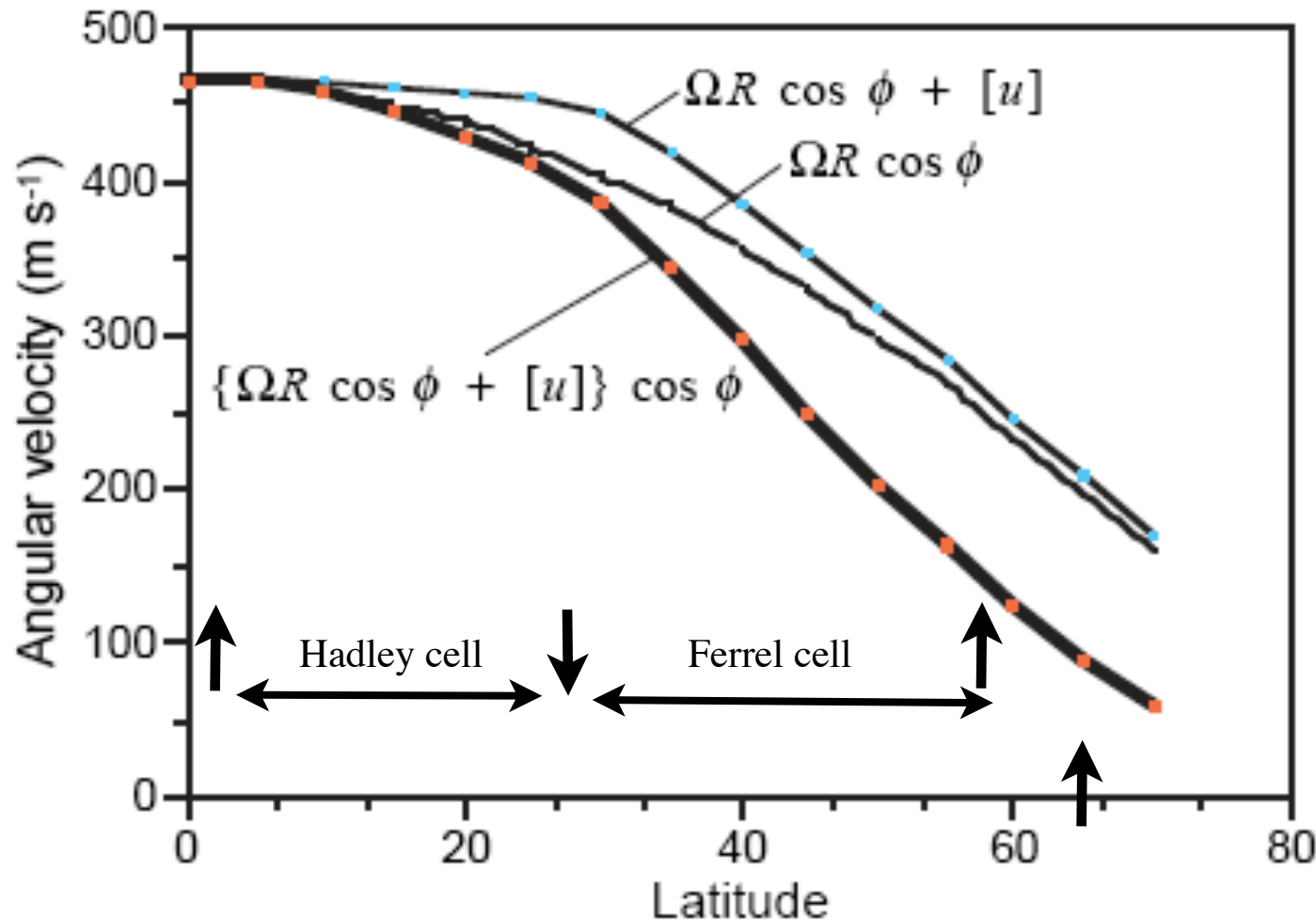
The eddies are not the answer

Scaling arguments: extratropical eddy fluxes are too small by a factor of  $Ro$

Extratropical eddy fluxes are upward; not downward



**So it must be the MMC**



$$\frac{2\pi R_E^2}{g} \int -[\bar{\omega}] (\Omega R_E \cos \phi + [u]) \cos^2 \phi dy$$

“Spin down” of the circulation in a teacup

The zonally averaged equation of motion

*Spherical geometry*

$$\frac{\partial [u]}{\partial t} = [v] \left( f - \frac{1}{\cos \phi} \frac{\partial}{\partial y} [u] \cos \phi \right) - [\omega] \frac{\partial [u]}{\partial p} - \frac{1}{\cos^2 \phi} \frac{\partial}{\partial \phi} [u^* v^*] \cos^2 \phi - \frac{\partial}{\partial p} [u^* \omega^*] + F_x$$

*Cartesian geometry*

$$\frac{\partial [u]}{\partial t} = [v] \left( f - \frac{\partial [u]}{\partial y} \right) - [\omega] \frac{\partial [u]}{\partial p} - \frac{\partial}{\partial y} [u^* v^*] - \frac{\partial}{\partial p} [u^* \omega^*] + F_x$$

*Neglecting vertical advection by MMC; using  $G$  to represent eddies*

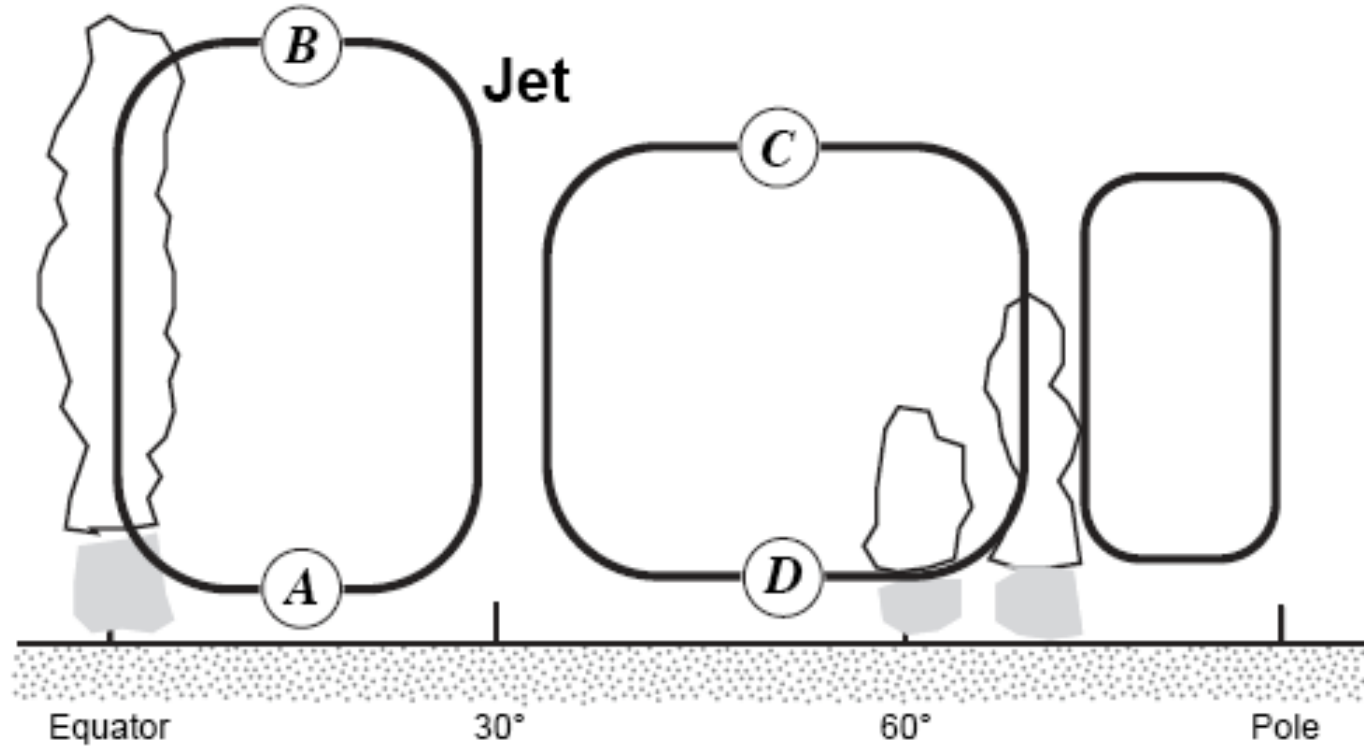
$$\frac{\partial [u]}{\partial t} = [v] \left( f - \frac{\partial [u]}{\partial y} \right) + G + F_x$$

$$\frac{\partial [u]}{\partial t} = [v] \left( f - \frac{\partial [u]}{\partial y} \right) + G + F_x$$

MMC	<i>dynamic stability</i>	eddy forcing	frictional drag
	$\propto dM/dy$		

For long term “balance requirement”  $d/dt = 0$

$$[v] = \frac{G + F_x}{f - \partial[u]/\partial y}$$

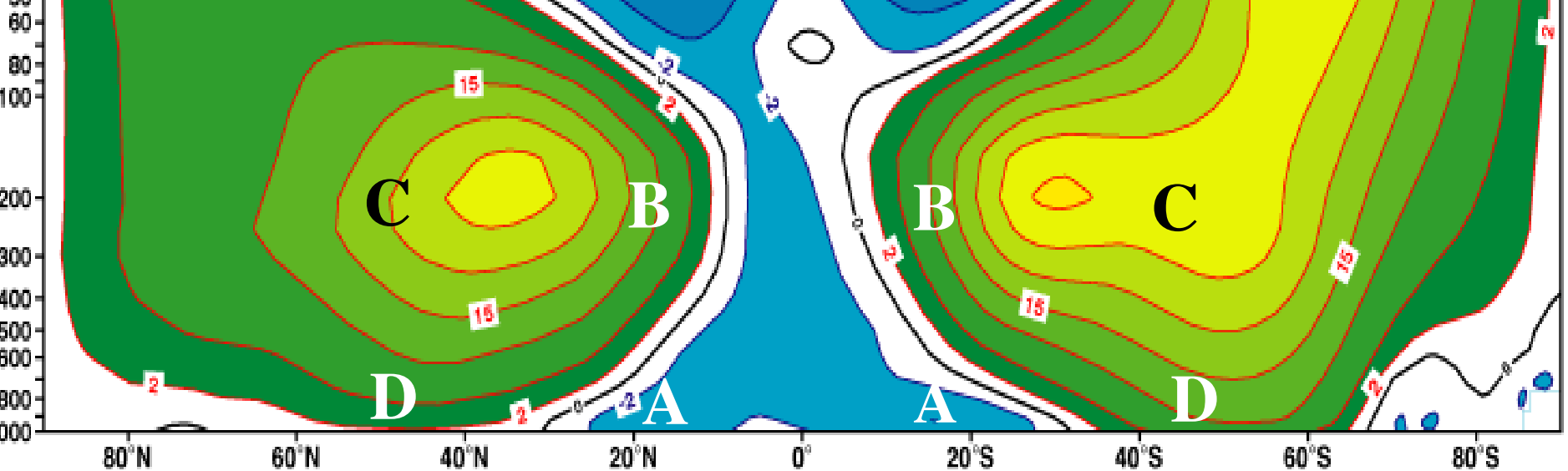


*tradewinds*

*westerlies*  
*storm track*

at A and D     $G = 0$

at B and C     $F = 0$



at **B**  $d[u]/dy \sim 30 \text{ m s}^{-1}$  over 2000 km  $\sim 1.5 \times 10^{-5} \text{ s}^{-1}$

$$f \sim 4 \times 10^{-5} \text{ s}^{-1}$$

$$f - d[u]/dy \sim 2.5 \times 10^{-5} \text{ s}^{-1}$$

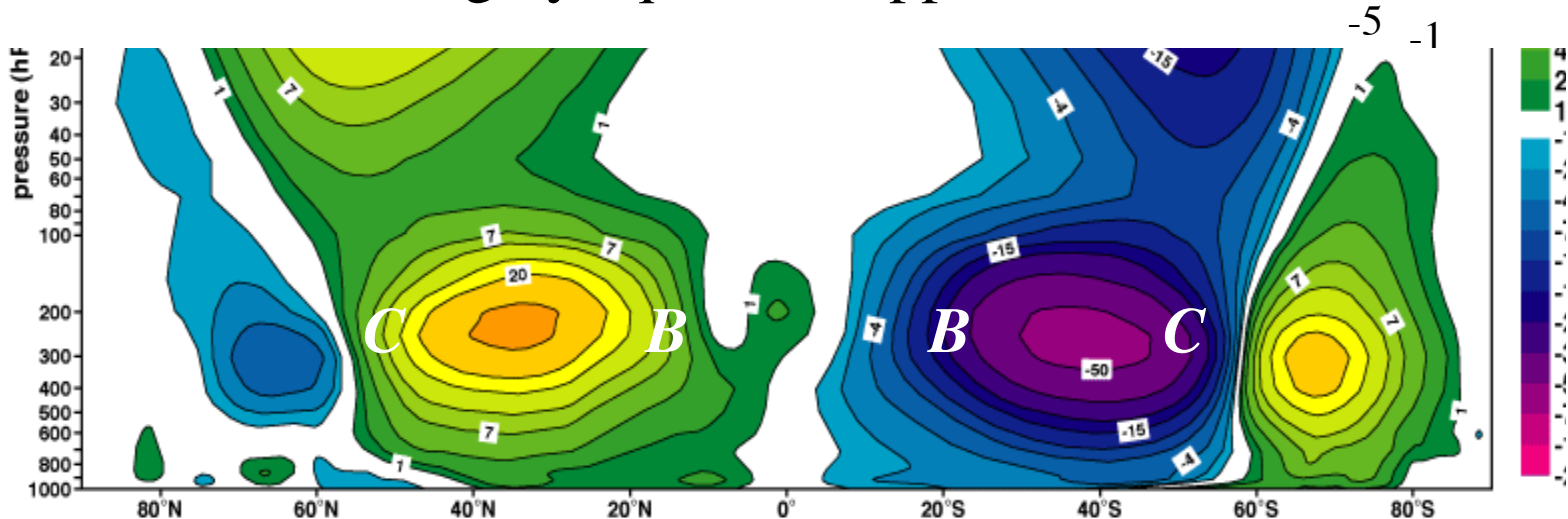
at **C**  $f - d[u]/dy \sim 10 \times 10^{-5} \text{ s}^{-1}$  4 × larger than at B

Recalling that

$$[\nu] = \frac{G + F_x}{f - \partial[u]/\partial y}$$

and  $F_x = 0$  at  $B$  and  $C$

and  $G$  is roughly equal and opposite at  $B$  and  $C$



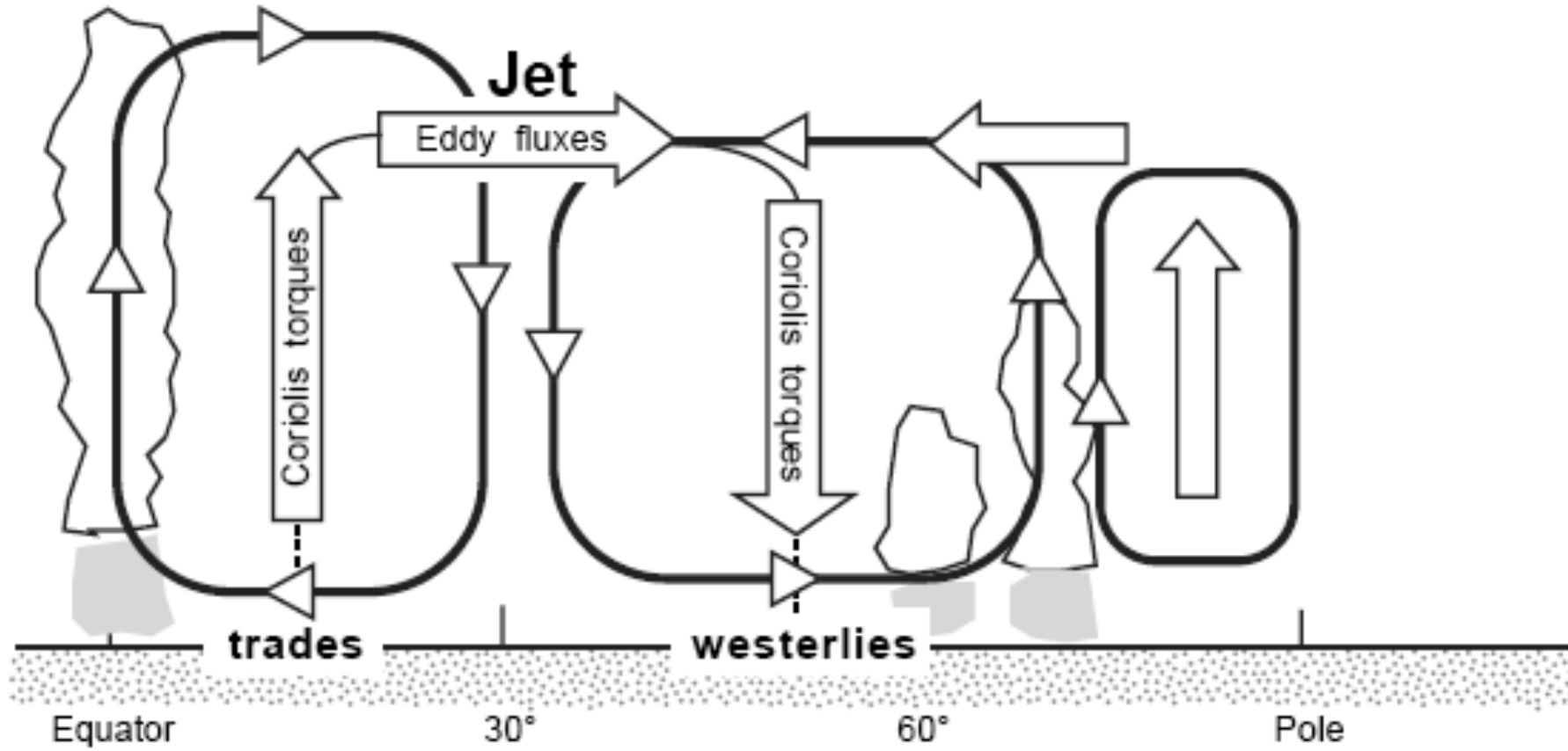
Recalling that

$$[\nu] = \frac{G + F_x}{f - \partial[u]/\partial y}$$

and  $F_x = 0$  at  $B$  and  $C$

and  $G$  is roughly comparable at  $B$  and  $C$

it follows that  $[\nu]$  is  $\sim 4 \times$  stronger at  $B$  than at  $C$   
i.e., that the Hadley cell is roughly 4 times as strong as the Ferrell cell



Note that we are able to prove the existence of Hadley and Ferrel cells and to reliably estimate their magnitudes without using observations of  $[v]$ . Until the 1980s, direct estimates of  $[v]$  were unreliable.